Physics – Uspekhi **44** (10) 999 – 1016 (2001)

REVIEWS OF TOPICAL PROBLEMS PACS numbers: **28.90.+t**, **44.25.+f**

Natural convection in heat-generating fluids

L A Bol'shov, P S Kondratenko, V F Strizhov

DOI: 10.1070/PU2001v044n10ABEH001012

Contents

Abstract. **Experimental and theoretical studies of convective heat transfer from a heat-generating fluid confined to a closed volume are reviewed. Theoretical results are inferred from analytical estimates based on the relevant conservation laws and the current understanding of the convective heat-transfer processes. Four basic and one asymptotic regime of heat transfer are identified depending on the heat generation rate. Limiting heat-transfer distribution patterns are found for the lower boundary. Heat transfer in a quasi-two-dimensional geometry is analyzed. Quasi-steady-state heat transfer from a cooling-down fluid without internal heat sources is studied separately. Experimental results and theoretical predictions are compared.**

L A Bol'shov Nuclear Safety Institute, Russian Academy of Sciences
Bol'shaya Tul'skaya 52, 113191 Moscow, Russian Federation
Tel. (7-095) 955-22 47. Fax (7-095) 958-00 40
E-mail: bolshov@ibrae.ac.ru
P S Kondratenko Nuclear Safety Institute, Russian Academy of Sciences
Bol'shaya Tul'skaya 52, 113191 Moscow, Russian Federation
Tel. (7-095) 955-22 91. Fax (7-095) 958-00 40
E-mail: kondrat@ibrae.ac.ru
V F Strizhov Nuclear Safety Institute, Russian Academy of Sciences
Bol'shaya Tul'skaya 52, 113191 Moscow, Russian Federation
Tel. (7-095) 955-22 08. Fax (7-095) 958-00 40
E-mail: vfs@ibrae.ac.ru

Received 10 May 2001
Uspekhi Fizicheskikh Nauk **171** (10) 1051 – 1070 (2001)
Translated by E Yankovsky; edited by A V Getling

1. Introduction

Bénard's experiment [1] and its theoretical interpretation proposed by Lord Rayleigh [2] marked the beginning of the century of research into natural convection in fluids (see Refs [3 – 13]). Commonly, investigators have concerned themselves with convection controlled by external boundary conditions (temperature differences), e.g. convection near a wall whose temperature differs from that of the fluid well apart from the wall. There is, however, a wide class of natural convection flows caused by internal heat sources rather than external conditions. For a long time such phenomena have received little attention. Only in the last quarter of the twentieth century interest in natural convection in fluids with internal heat sources has been stimulated by the demands of nuclear power engineering. The importance of this research became especially evident after the accidents at the Three Mile Island and Chernobyl atomic power stations; as a result, the problem of safety in atomic power engineering became an independent field of research.

In analyzing the scenarios and predicting the consequences of severe accidents involving reactor core degradation in nuclear power plants, the problem emerges as to the confinement of hot radioactive melt within the reactor vessel. At present, the most acceptable solution to this problem for low- and medium-power reactors is the cooling of the reactor vessel externally, by boiling water [14]. In view of this, it becomes extremely important to know the regularities of the the distribution of heat release by a fluid with internal heat sources that is confined to a closed volume. Such regularities are mainly studied using laboratory modeling [15 – 31] and numerical [32–37] simulations. When the heat release is high and corresponds to real situations related to the safety of nuclear reactors, the convective flow of a fluid becomes highly turbulent, and therefore numerical simulation techniques encounter serious difficulties. This makes analytical approaches especially important.

A consistent theory of turbulence is not yet available, and the only way to derive the analytical laws governing convection in fluids with a high heat release is to obtain qualitative estimates from the general principles related to symmetry properties, conservation laws, and similarity and dimensionality considerations. The method of estimates allows us to determine the type of a functional dependence, but cannot accurately evaluate the numerical factors. In this respect, this method is weaker than a direct computer simulation. However, in contrast to the latter, this method makes it possible to extend the research in natural convection to the region of parameters where computer simulation is helpless.

The method of analytical estimates in hydrodynamics in general and in the theory of convective heat transfer in particular traces back to the classical works of Prandtl [3, 4], von Kármán [5], Kolmogorov [6], Landau [7], and Zel'dovich [8]. All these researchers studied fluids without internal heat sources. Only recently this approach came to use in studying fluids with such sources [38–44].

The aim of the present review is to give an idea of the current state of experimental and theoretical (based on analytical estimates) studies of convective heat transfer from a one-component fluid with internal heat sources.

Several remarks concerning the layout of our presentation are in order. The main characteristics of heat transfer from a fluid with internal heat sources are the distribution of the heat flux density at the boundary, q, and the maximum excess of the bulk temperature of the fluid over the boundary's temperature, ΔT. It is convenient to represent the laws related to these characteristics in the form of dependences of the dimensionless Nusselt and Rayleigh numbers (Nu and Ra), defined as

$$q = \frac{\lambda \Delta T}{H} \, \mathrm{Nu} \,, \tag{1.1}$$

$$\mathrm{Ra} = \frac{g\alpha \Delta T H^3}{\nu\chi} \,, \tag{1.2}$$

on the modified Rayleigh number

$$\mathrm{Ra}_{\mathrm{i}} = \frac{g\alpha Q H^5}{\lambda \nu \chi} \,. \tag{1.3}$$

Here λ, ν, χ, and α are, respectively, the heat conductivity, the kinematic viscosity, the thermal diffusivity, and the thermal volumetric expansion coefficient of the fluid; H is the characteristic vertical dimension (height) of the volume occupied by the fluid; g is the acceleration due to gravity; and Q is the power density of the internal heat sources, whose distribution is assumed to be homogeneous. Naturally, the Nusselt number Nu, which characterizes the heat flux distribution over the boundary, is a function of coordinates at the bounding surface, while the number Ra_{i} is actually the dimensionless strength of internal heat release in the fluid.

Note that the number Ra for a fluid without internal heat sources is an independent variable [here ΔT in (1.2) should be interpreted as the characteristic temperature difference related to the boundary conditions]. Accordingly, heat transfer in such a fluid is a function of Ra, $\mathrm{Nu} = \mathrm{Nu}(\mathrm{Ra})$. In a heat generating fluid, however, Ra_{i} is an independent variable, while Ra should be determined, being (together with Nu, as noted earlier) a function of Ra_{i}, i.e. $\mathrm{Nu} = \mathrm{Nu}(\mathrm{Ra}_{\mathrm{i}})$ and $\mathrm{Ra} = \mathrm{Ra}(\mathrm{Ra}_{\mathrm{i}})$.

The plan of the review is as follows. In Section 2 we present the results of the most widely known experiments on heat transfer by fluids with internal heat sources. Section 3 describes the analytical results for integral heat-transfer characteristics, which determine the distribution of the heat flux between the lower and upper boundaries of the fluid volume. From the practical viewpoint, the relationship between the heat fluxes through the upper and lower boundaries is important due to the difference in the modes of heat removal in severe accidents at nuclear power plants: heat is removed by hot water from the lower part of the reactor vessel, while the upper part is cooled through radiative heat exchange. In Section 4 we discuss details of the heat flux distribution over the lower boundary, which are important in evaluating the possibilities for external cooling. In most model experiments, the original, prototype volume filled with a fluid is represented by a thin, plane section passing through the vertical axis of this volume. This section is called a quasi-two-dimensional, or slice volume. The question of whether such a quasi-two-dimensional volume can be used to model natural convection in the prototype three-dimensional, axisymmetric volume is considered in Section 5. One approach to the experimental modeling of heat transfer from a heat-generating fluid consists in studying the quasi-steady-state process of cooling of a fluid without internal heat sources. A theoretical analysis of the heat transfer from such a fluid is presented in Section 6. In Section 7 we summarize the results.

2. A review of experiments modeling heat transfer

The experimental investigations in modeling heat transfer from a heat-generating fluid confined to a closed volume differ both in geometry and in the setup of the experiment. Axisymmetric containers filled with a heat-generating fluid and bounded by a horizontal upper surface are of interest from the practical viewpoint.

In most experiments conducted so far, the bulk heat release is brought about by passing a direct current or by microwaving. However, these methods lead to difficulties in ensuring homogeneity in heat release. A way to overcome these difficulties is to make the linear size of the volume in one of the three directions much smaller than the other two sizes, i.e., to choose a thin, plane-parallel horizontal or vertical layer. A thin vertical layer is usually interpreted as the central vertical slice of the prototype three-dimensional volume. In experiments using such geometry, the fluid is cooled through the narrow sections of the boundary at a constant temperature, while the wide vertical sections are thermally insulated. It is assumed that in such geometry the heat-flux distribution over the cooled sections of the boundary of the container reproduces the heat-removal distribution in the prototype volume of the fluid with internal heat sources. The quasi-two-dimensional model volume is characterized in this case by three length parameters — the vertical size (height) H, the larger horizontal size D, and the layer thickness (the smaller horizontal size) L.

A different experimental approach to modeling heat removal from a fluid with internal heat sources consists in studying quasi-steady-state heat transfer from a cooling-down fluid without internal heat sources.

The experimental results discussed in the present review can be divided into two groups. The first group consists of experiments in which the heat-release rates are moderate and correspond to modified Rayleigh numbers $\mathrm{Ra_i} < 10^{12}$ or $\mathrm{Ra_i} \sim 10^{12}$ (Section 2.1), while the second group includes experiments with extremely high heat-release rates, $\mathrm{Ra_i} > 10^{12}$ (Section 2.2).

2.1 Moderate heat-release rates

A plane horizontal layer with isothermal top and bottom boundaries. Kulacki and Goldstein [15] modeled a natural convective flow of a fluid in a rectangular parallelepiped with a square horizontal base, under adiabatic conditions at all sidewalls. The side length of the base was 25.4 cm, and the height of the fluid layer in the container varied from 1.27 to 6.35 cm. An aqueous solution of silver nitrate with a concentration of 0.02 mol % was used as the working fluid. Bulk heat release was brought about by transmitting a direct electric current through the salt solution. The upper and lower sections of the boundary of the container were made of copper plates. The vertical temperature profile was measured by a laser interferometer, with the laser beam sent in the horizontal direction perpendicular to the applied potential difference. The dimensionless heat-transfer coefficient, the Nusselt number, was determined from measurements of the vertical temperature profile in the central section of the container.

The results of these experiments were represented in the form of empirical relations for the Nusselt numbers describing the heat transfer through the upper (up) and lower (dn) sections of the boundary:

$$\mathrm{Nu_{up}} = 0.371\,\mathrm{Ra_i^{0.228}}\,, \quad \mathrm{Nu_{dn}} = 1.407\,\mathrm{Ra_i^{0.095}}\,;$$
$$7.1 \times 10^4 \leqslant \mathrm{Ra_i} \leqslant 2.4 \times 10^7\,, \quad 0.05 \leqslant \frac{H}{D} \leqslant 0.25\,. \tag{2.1}$$

The errors in the results were estimated to be $\pm 10\%$.

Mayinger et al. [16] studied heat transfer in plane horizontal layers with a square $14 \times 14\ \mathrm{cm}^2$ base and height varying from 0.5 to 6 cm. The results were represented as follows:

$$\mathrm{Nu_{up}} = 0.345\,\mathrm{Ra_i^{0.233}}\,, \quad \mathrm{Nu_{dn}} = 1.389\,\mathrm{Ra_i^{0.095}}\,;$$
$$4.0 \times 10^4 \leqslant \mathrm{Ra_i} \leqslant 5.0 \times 10^{10}\,, \quad 0.05 \leqslant \frac{H}{D} \leqslant 0.43\,. \tag{2.2}$$

A plane horizontal layer with an isothermal top boundary and a thermally insulated bottom boundary. Kulacki and Emara [17] studied the heat transfer from a plane horizontal layer with a cooled top boundary, adiabatic bottom boundary, and adiabatic sidewalls, over a broad range of Rayleigh numbers (up to 4.4×10^{12}), including a sizable interval corresponding to turbulent convection. Two containers with horizontal square bases were used, with side lengths of 25.4 and 50.8 cm. The results were given in the following form:

$$\mathrm{Nu_{up}} = 0.338\,\mathrm{Ra_i^{0.227}}\,, \quad 3.8 \times 10^3 < \mathrm{Ra_i} < 4.3 \times 10^{12}\,,$$
$$0.025 < \frac{H}{D} < 0.5\,. \tag{2.3}$$

Note that Kulacki and Nagle [18] also studied convection in a plane horizontal layer with a thermally insulated bottom.

Vertically oriented containers: rectangular geometry. Mayinger et al. [16, 20] and Jahn [19] measured the heat transfer in a rectangular parallelepiped that is thin in one horizontal direction. The width of the container in the other horizontal direction was $D = 2-6$ cm. All the four narrow faces of the parallelepiped were cooled, while the two broad vertical walls were thermally insulated. The heat transfer through the upper face, narrow sidewalls (sd), and lower face was found to be of the form:

$$\mathrm{Nu_{up}} = 0.345\,\mathrm{Ra_i^{0.233}}\,, \quad \mathrm{Nu_{sd}} = 0.6\,\mathrm{Ra_i^{0.19}}\,,$$
$$\mathrm{Nu_{dn}} = 1.389\,\mathrm{Ra_i^{0.095}}\,;$$
$$3 \times 10^7 < \mathrm{Ra_i} < 5.0 \times 10^{10}\,, \quad 0.05 < \frac{H}{D} < 0.5\,. \tag{2.4}$$

Note that the additional cooling of the sidewalls did not change the heat-transfer coefficients $\mathrm{Nu_{up}}$ and $\mathrm{Nu_{dn}}$ [cf. (2.2)]. The dependence of the heat transfer on the thickness of the parallelepiped was not studied, but was assumed to be very weak.

In their experiments, Stainbrenner and Reineke [21] studied heat transfer in thin, square-shaped vertical layers. The side of the square was 80 cm, and the layer thickness was $L = 3.5$ cm. The wide vertical walls were made of glass and were thermally insulated. The optical probing of the fluid was done along the normal to these walls. Boundary conditions of two types were used: they corresponded to the cooling of either only the narrow sidewalls or all the narrow sections of the boundary. The same temperature was maintained at all the cooled surfaces. The heat transfer through the sidewalls (sd) was approximated as follows:

$$\mathrm{Nu_{sd}} = 0.85\,\mathrm{Ra_i^{0.19}}\,; \tag{2.5}$$
$$5 \times 10^{12} \leqslant \mathrm{Ra_i} \leqslant 1.0 \times 10^{14}\,, \quad \frac{H}{D} = 1\,, \quad \frac{L}{H} = 0.044\,.$$

The data on the heat transfer through the upper and lower boundaries proved to be in good agreement with Jahn's results [19] [see (2.4)].

Vertically oriented containers: semicylindrical geometry. Mayinger et al. [16, 20] and Jahn [19] also studied the heat transfer in the geometry of a short semicylinder with a horizontal axis and a plane horizontal upper boundary. The radius of the cylindrical segment was $R = 2.5-28$ cm. The upper horizontal boundary and the lower curved boundary were cooled. The broad vertical thermally insulated sections of the boundary were used as electrodes for electric current. The researchers studied the heat transfer as a function of the height H of the fluid in the cylindrical segment. The results led to the following relationship between the Nusselt number and the modified Rayleigh number:

$$\mathrm{Nu_{up}} = 0.36\,\mathrm{Ra_i^{0.23}}\,, \quad \mathrm{Nu_{dn}} = 0.54\,\mathrm{Ra_i^{0.18}}\left(\frac{H}{R}\right)^{0.26}\,;$$
$$10^7 < \mathrm{Ra_i} < 5.0 \times 10^{10}\,, \quad 0.3 < \frac{H}{R} < 1.0\,. \tag{2.6}$$

The researchers also studied the heat-transfer distribution over the lower section of the boundary. They found that the heat transfer in the vicinity of the lowest point of the boundary differs substantially from purely molecular heat transfer (i.e. without convection), while in the upper part of the lateral surface it is close to that at the upper horizontal boundary.

2.2 Very high heat-release rates

Experiments with the BAFOND facility. Alvarez et al. [22] studied heat removal from a weak aqueous solution of salt that filled a vertical cylinder at whose boundary the temperature was maintained constant. The heat release in the solution was maintained transmitting an electric current between the upper and lower round horizontal bases of the cylinder. The measurements were carried out at heat release rates up to a level corresponding to $\mathrm{Ra}_i \approx 10^{16}$. It was found that a simple model could describe the experimental data. According to this model, the distribution of the heat flux to the vertical section of the boundary is determined by the well-known formulas [45] that describe the behavior of a laminar boundary layer at fairly small Rayleigh numbers, with $\mathrm{Nu} \sim \mathrm{Ra}^{1/4}$, and of a turbulent boundary layer at larger Rayleigh numbers, with $\mathrm{Nu} \sim \mathrm{Ra}^{1/3}$. For intermediate values of the Rayleigh number ($\mathrm{Ra}_i \approx 10^{13}$) both formulas describe the results of measurements quite well. On this basis, Alvarez et al. [22] claim that at Rayleigh numbers $\mathrm{Ra}_i \approx 10^{13}$ the flow regime in the boundary layer near the vertical section of the boundary changes from laminar to turbulent.

Experiments with the UCLA facility. Asfia and Dhir [23] and Frantz and Dhir [24] studied heat and mass transfer in a three-dimensional hemispherical geometry. The inner diameters of the hemispheres were 44.21 and 15.2 cm. Bulk heat release was produced by applying a microwave field.The uniformity of heat release was controlled by recording the growth of temperature at different points inside the hemisphere. The measurements were done at modified Rayleigh numbers $\mathrm{Ra}_i \lesssim 10^{14}$.

It was found that under adiabatic conditions at the upper horizontal section of the boundary the heat transfer through the lower boundary satisfies a relationship close to that obtained by Mayinger et al. [16, 20] [see (2.6)]:

$$\mathrm{Nu}_{\mathrm{dn}} = 0.5\,\mathrm{Ra}_i^{0.2}\left(\frac{H}{R}\right)^{0.25}. \tag{2.7}$$

Here H is the level of the fluid in the hemisphere.

Experiments with the COPO facility. Kymäläinen et al. [25, 26] used the COPO facility to study heat transfer at large Rayleigh numbers (up to 1.7×10^{15}) in a quasi-two-dimensional geometry. On a 1 : 2 scale, the facility reproduces the VVER 440 reactor vessel with a semielliptical bottom and a vertical cylindrical section. The slice thickness amounted to 10 cm. The wide vertical sections of the boundary were made of polycarbonate with holes for optical measurements. The height of the fluid varied from 60 to 80 cm, and the width D was 1.77 m. An aqueous solution of zinc sulfate was used as the working fluid. Bulk heat release was produced by transmitting a direct electric current through the salt solution. The peak voltage amounted to 30 kV and the peak power to 6 kW. The maximum operating temperature was 80 °C. Fifty-seven cooling elements were used to cool the narrow lateral and bottom sections of the boundary. The temperature was controlled using thermocouples. These experiments made it possible to determine the heat transfer and compare it to the results of earlier studies, e.g. those done by Stainbrenner and Reineke [21].

The researchers found that about 70% of the energy input was removed by heat transfer through the upper horizontal boundary, while the remainder was removed through the lateral and bottom sections of the boundary. They also found that the heat transfer through the vertical walls obeys Stainbrenner and Reineke's formulas [21] extrapolated to larger Rayleigh numbers, the heat transfer through the upper boundary is somewhat larger, and the heat transfer through the bottom section of the boundary is much smaller than the value predicted by Stainbrenner and Reineke's formulas [21] if the height of the fluid level is assumed to be the characteristic height. For this reason, in analyzing the heat transfer through the lower boundary, the height of the curved part of the container, H_c, was taken as the length scale. As a result, the formulas describing the experimental data gathered by Kymäläinen et al. [25, 26] assume the form

$$\begin{gathered}\mathrm{Nu}_{\mathrm{up}} = 0.345\,\mathrm{Ra}_i^{0.233}, \quad \mathrm{Nu}_{\mathrm{sd}} = 0.85\,\mathrm{Ra}_i^{0.19},\\ \mathrm{Nu}_{\mathrm{dn}} = 0.54\,\mathrm{Ra}_i^{0.18}\left(\frac{H_c}{R}\right)^{0.26};\\ 4\times 10^{12} < \mathrm{Ra}_i < 1.7\times 10^{15}.\end{gathered} \tag{2.8}$$

Helle et al. [27] conducted additional experimental studies using the COPO – COPO II facility. An important modification consisted in cooling the outer boundary with liquid nitrogen, which led the to formation of a crust on the inner boundary of the volume and thus ensured ideally isothermal boundary conditions. Containers of two different geometries were used. The first container had a semielliptical bottom part with a vertical cylindrical section (this corresponded in shape to the bottom of a VVER 440 reactor) and the second one had a hemispherical bottom part (corresponding in shape to the AP 600 reactor vessel). In both cases the facility reproduces the vessel on a 1 : 2 scale. The results were compared with those obtained in the first series of experiments (COPO I; see Refs [25, 26]) and with the empirical relationships known from earlier studies. The average heat transfer through the upper boundary proved to be close to the value obtained from Stainbrenner and Reineke's correlation [21] and to the COPO I results, irrespective of the container shape. However, the average heat transfer through the lower boundary in the COPO II experiments was higher than in the first series of experiments. Moreover, the COPO II experiments revealed a strong dependence of the heat flux at the lower boundary on the polar angle θ (this angle gives the angular distance along the boundary from the lowest point, the pole, measured upward; see Section 4 below).

Experiments with the BALI facility. The BALI program, initiated by Bonnet et al. [28], is intended for studying heat and mass transfer in large volumes of water and for modeling convection in a reactor on a 1 : 1 scale. The facility corresponds to a semicircle with a quasi-two-dimensional geometry, 2 m in radius and 0.15 m thick. The Rayleigh number in these experiments varied from 10^{15} to 10^{17}, covering the region most important for the problem of safety of nuclear reactors. The results were represented by the following relationships:

$$\mathrm{Nu}_{\mathrm{up}} = 0.383\,\mathrm{Ra}_i^{0.233}, \quad \mathrm{Nu}_{\mathrm{dn}} = 0.116\,\mathrm{Ra}_i^{0.25}\left(\frac{H}{R}\right)^{0.32}. \tag{2.9}$$

In addition to measuring the heat flux distribution at the boundary, the researchers recorded the temperature distribution along the axis of the modeling cavity. It was found that this distribution is uniform in the upper part of the container when averaged over time, while in the lower part the time-averaged distribution is stably stratified. For very large values of $\mathrm{Ra_i}$ the thermally uniform upper region occupies less than one-third of the entire volume in height.

Note that the dependence of $\mathrm{Nu_{dn}}$ on H/R in (2.9) agrees with the earlier result of Mayinger et al. [16, 19] for a quasi-two-dimensional volume, (2.5), and with Asfia and Dhir's result [23] for a hemisphere, (2.7); these relationships contain the ratio H/R to the powers 0.26 and 0.25, respectively.

Experiments with the mini-ACOPO facility. The mini-ACOPO facility designed by Theofanous and Liu [29] exists in two versions (A and B) and is used to verify the main laws governing natural convection, which were established in earlier experiments for smaller Rayleigh numbers, and also to establish the role of the Prandtl number $\mathrm{Pr} = \nu/\chi$. The shape of the model container was hemispherical. The approach used in these experiments differs substantially from the earlier approaches. Instead of a fluid with a bulk heat release, the heat transfer from a cooling fluid without internal heat sources was studied. It was assumed that at each moment the quasi-steady state of the cooling fluid reproduced exactly the corresponding steady state of a fluid with internal heat sources. This assumption was based on the fact that the boundary-layer processes that determine the characteristics of heat transfer are much faster than the cooling itself. The working fluid in version A was Freon 113, with which a hemispherical container of radius 22 cm was filled. Ten cooling elements were used to maintain the required temperature conditions. In version B the working fluid was water. Studies of the local heat flux distribution were not planned for this version, so that the cooling system was simpler in this case.

A comparison of the heat transfer through the boundary with the calculations of the total variation of the thermal energy within the volume of the cooling fluid showed that in most tests an energy balance held to an accuracy of no less than 10%. The typical duration of one series of measurements was 15 to 30 min, depending on the cooling rate.

In eight tests with setup version A, the initial Freon temperature was approximately 40 °C, while the temperature at the boundary was close to 3 °C. In the course of one cooling cycle, the modified Rayleigh number corresponding to the given experiment varied from 2×10^{13} to 7×10^{14} and the Prandtl number from 7 to 11. In the three tests with version B, the initial temperature of the cooling fluid (water) was close to 100 °C, the cooling circuit operated at 3, 26, and 66 °C, the range of variation was $2 \times 10^{12} < \mathrm{Ra_i} < 3 \times 10^{13}$ for the modified Rayleigh number and $2.5 < \mathrm{Pr} < 11.0$ for the Prandtl number.

The measured heat transfer through the upper boundary were found to agree very well with Stainbrenner and Reineke's correlation [21] over the entire range of modified Rayleigh numbers. The heat transfer through the lower boundary was represented by the following formulas:

$$\mathrm{Nu_{dn}} = 0.048\,\mathrm{Ra_i^{0.27}}\,, \quad \mathrm{Nu_{dn}} = 0.0038\,\mathrm{Ra_i^{0.35}}\,,$$
$$10^{12} \leqslant \mathrm{Ra_i} \leqslant 3 \times 10^{13}\,; \quad 3 \times 10^{13} \leqslant \mathrm{Ra_i} \leqslant 7 \times 10^{14}\,. \tag{2.10}$$

An important feature of these results is that at $\mathrm{Ra_i} \approx 3 \times 10^{13}$ a transition to larger exponents takes place.

The measured local polar-angle distributions of the heat flux at the lower boundary were represented as follows:

$$\frac{\mathrm{Nu_{dn}}(\theta)}{\mathrm{Nu_{dn}}} = 0.1 + 1.08\left(\frac{\theta}{\theta_p}\right) - 4.51\left(\frac{\theta}{\theta_p}\right)^2 + 8.61\left(\frac{\theta}{\theta_p}\right)^3,$$
$$0.1 \leqslant \frac{\theta}{\theta_p} \leqslant 0.6\,,$$
$$\frac{\mathrm{Nu_{dn}}(\theta)}{\mathrm{Nu_{dn}}} = 0.41 + 0.35\left(\frac{\theta}{\theta_p}\right) + \left(\frac{\theta}{\theta_p}\right)^2,$$
$$0.6 \leqslant \frac{\theta}{\theta_p} \leqslant 1.0\,, \quad \theta_p = \frac{\pi}{2}\,. \tag{2.11}$$

An important consequence of these results is that the heat transfer is independent of the Prandtl number within the interval from 2.5 to 10.8.

Experiments with the ACOPO facility. Theofanous et al. [30, 31] conducted their experiments with the ACOPO facility using the same approach as in the case of the mini-ACOPO facility. However, owing to the larger size of the model container (a diameter of 2 m, i.e., half the reactor diameter), it was possible to reach a Rayleigh number of 10^{16}. The working fluid in these experiments was water with an initial temperature of 100 °C, and a temperature of 0 °C was maintained at the boundary. The following correlations for heat transfer (different from those known from earlier experiments) were obtained:

$$\mathrm{Nu_{up}} = 1.95\,\mathrm{Ra_i^{0.18}}\,, \quad \mathrm{Nu_{dn}} = 0.3\,\mathrm{Ra_i^{0.22}}\,. \tag{2.12}$$

3. Integral laws governing heat transfer

3.1 General physical picture

Let the container of volume V filled with a heat-generating fluid (depicted schematically in Fig. 1) have the shape of a body of revolution about a vertical axis and a plane upper (horizontal) section of the boundary with an area of S_{up}. We denote the remaining (lower) part of the boundary by S_{dn}. The entire boundary S of the volume is assumed to be rigid and isothermal. The vertical size (height) of the volume is denoted by H.

The general picture of convective heat transfer can be described as follows.

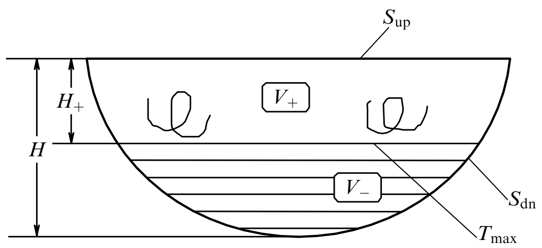

Figure 1. Central vertical section of the volume filled with the fluid: S_{up} and S_{dn} are, respectively, the upper horizontal boundary and the lower curved boundary; T_{max} designates the horizontal plane that passes through the point of the highest temperature in the volume; V_+ and V_- are the parts of the volume above and below the plane T_{max}; H is the vertical size (height) of the entire volume; and H_+ is the height of V_+.

The horizontal plane passing through the point of the highest time-averaged temperature separates the volume V into two portions. In the region V_+ of height H_+, in view of the inverse temperature distribution, the situation resembles the conditions needed for Rayleigh – Bénard (RB) convection to set in [1, 2]. A natural RB convective flow transfers heat to the horizontal section of the boundary, $S_{\rm up}$. The heat transport to the lower boundary $S_{\rm dn}$ is determined by a boundary layer, thin compared to H, where the fluid flows downward. A slow reverse flow of the fluid under conditions with a positive vertical temperature gradient does not prevent the system from the formation of a stable temperature stratification outside the boundary layer in the lower part of the volume, V_-.

In this section we will discuss the integral laws that govern heat transfer, i.e. the heat fluxes averaged over $S_{\rm up}$ and $S_{\rm dn}$. We derive these laws on the basis of the general condition for energy balance and from the fragmentary similarity in heat transfer between fluids with and without internal heat sources.

3.2 Condition for energy balance

The condition for steady-state energy balance in a fluid with uniformly distributed heat sources of volume power density Q can be written as

$$\frac{\lambda \Delta T}{H} \int_S \mathrm{d}S\,\mathrm{Nu} = QV\,, \quad S = S_{\rm up} + S_{\rm dn}\,. \tag{3.1}$$

We express ΔT and Q in terms of the ordinary and the modified Rayleigh number [equations (1.2) and (1.3)] to arrive at the following relationship:

$$\mathrm{Ra}\,\overline{\mathrm{Nu}} = \mathrm{Ra_i}\,. \tag{3.2}$$

Here $\overline{\mathrm{Nu}}$ is the Nusselt number averaged over the entire boundary and is given by the formula

$$\overline{\mathrm{Nu}} = \frac{H}{V}(S_{\rm up}\mathrm{Nu}_{\rm up} + S_{\rm dn}\mathrm{Nu}_{\rm dn})\,, \tag{3.3}$$

where

$$\mathrm{Nu}_i = \frac{1}{S_i}\int_{S_i} \mathrm{d}S\,\mathrm{Nu}\,, \quad i = \mathrm{up}, \mathrm{dn} \tag{3.4}$$

are the Nusselt numbers averaged over the upper and the lower boundary.

Usually the theoretical laws for heat transfer and the corresponding results of experiments and numerical simulations are represented by power functions. We define the exponents γ_i, β_i ($i = \mathrm{up}, \mathrm{dn}$), β, and ε as follows:

$$\mathrm{Nu}_i \propto \mathrm{Ra_i}^{\gamma_i}\,, \quad \mathrm{Nu}_i \propto \mathrm{Ra}^{\beta_i}\,,$$
$$\overline{\mathrm{Nu}} \propto \mathrm{Ra}^{\beta}\,, \quad \mathrm{Ra} \propto \mathrm{Ra_i}^{\varepsilon}\,, \tag{3.5}$$

where we have omitted the numerical factors of order unity.

The substitution of (3.5) into (3.2) leads to the following important relations between various exponents:

$$\varepsilon = (1+\beta)^{-1}\,, \tag{3.6}$$

$$\gamma_i = \frac{\beta_i}{1+\beta}\,. \tag{3.7}$$

We should now determine the exponents $\gamma_{\rm up}$, $\gamma_{\rm dn}$, and ε, abstracting from the numerical factors of the power laws (they are of order unity; determining these factors is impossible within the framework of the semiquantitative theory discussed here). We assume that the Prandtl number is greater than or of order unity, $\mathrm{Pr} \geqslant 1$.

Note that the laws (3.5) with constant exponents are valid within restricted intervals of $\mathrm{Ra_i}$ that correspond to certain combinations of regimes of heat transfer through $S_{\rm up}$ and $S_{\rm dn}$. Transitions between these regimes result in changes (abrupt or gradual) in the exponents.

3.3 Basic heat-transfer regimes

When analyzing heat transfer in heat-generating fluids, we use similarities to the case of a fluid without heat sources. Firstly, there is an analogy between convection in volume V_+ and RB convection. Secondly, there is close similarity between the boundary layers in the problem at hand and near a cooled surface. These analogies can be substantiated by the following ideas. In the region of large Rayleigh numbers, $\mathrm{Ra} \gg 1$, we are interested in, most of the heat resistance in the process of heat transfer to the boundary is due to thin thermal boundary layers. The thickness of these layers is much smaller than the characteristic linear size of the entire fluid volume — the height H. Hence the power of heat release in these layers is negligible compared to the heat fluxes passing through them. This implies that heat generation in these layers has virtually no effect on their structure and, accordingly, on the heat-transfer characteristics. Below we list the main characteristics of heat transfer regimes for a fluid without internal heat sources (RB convection and a boundary layer), which are prototypes of the characteristics for a heat-generating fluid.

RB convection in a plane horizontal fluid layer of height H_+, heated from below, exhibits the following heat-transfer regimes, which differ in the exponent $\beta_{\rm RB}$ in the relationship for the Nusselt number:

$$\mathrm{Nu_{RB}} \propto \mathrm{Ra}_+^{\beta_{\rm RB}}\,, \tag{3.8}$$

where $\mathrm{Ra}_+ = \mathrm{Ra}(H \to H_+)$. Within the interval $\mathrm{Ra_{c1}} < \mathrm{Ra} < \mathrm{Ra_{c2}}$, convection is laminar and $\beta_{\rm RB} = 1/4$ [46]. In the interval $\mathrm{Ra_{c2}} < \mathrm{Ra} < \mathrm{Ra_{c3}}$, soft turbulence is present and $\beta_{\rm RB} = 1/3$ [47]. Finally, for Rayleigh numbers $\mathrm{Ra} > \mathrm{Ra_{c3}}$ we have hard turbulence with $\beta_{\rm RB} = 2/7$ [47]. The critical values $\mathrm{Ra_{c1}}$, $\mathrm{Ra_{c2}}$, and $\mathrm{Ra_{c3}}$ depend on the aspect ratio $A = D/H_+$, where D is the horizontal size of an RB cell. For $A > 1$, $\mathrm{Ra_{c1}} \sim 10^3$. For $A \approx 1$, we have $\mathrm{Ra_{c2}} = 2 \times 10^5$ and $\mathrm{Ra_{c3}} \simeq 4 \times 10^7$ [47]. If $A = 6.5$, $\mathrm{Ra_{c3}} \simeq 10^4$ [48]. In view of this, we can assume that, at sufficiently high aspect ratios, as Ra_+ is increased, at $\mathrm{Ra}_+ > \mathrm{Ra_{c1}}$ the laminar flow regime in an RB layer undergoes a transition directly to the hard turbulence regime, skipping the soft turbulence regime, which is not realized in this case.

The boundary layer at the vertical wall in a fluid without internal heat sources, which is a prototype for the boundary layer at the section $S_{\rm dn}$ of the boundary of a cavity filled with a heat-generating fluid, may be in two heat-transfer regimes, which differ in the value of the exponent of the power law for the Nusselt number:

$$\mathrm{Nu_{bl}} \propto \mathrm{Ra}^{\beta_{\rm bl}}\,. \tag{3.9}$$

These are the laminar regimes with $\beta_{\rm bl} = 1/4$ [13] and the turbulent regime with $\beta_{\rm bl} = 1/3$ [49]. The transition between these two regimes occurs at the critical value of the Rayleigh number, $\mathrm{Ra} = \mathrm{Ra}^*$, which depends on the Prandtl number. According to theoretical estimates made by Bejan and

Gunnington [50], for $\mathrm{Pr} > 1$ this dependence has the form $\mathrm{Ra}^* \propto \mathrm{Pr}^2$. At the same time, as suggested by experiments, the numerical factor in this relationship varies from one experiment to another by two orders of magnitude [51, 52]. This may even out the dependence if the variations of the Prandtl number are not too wide. Note that according to experimental data, the value of the critical Rayleigh number for the transition between regimes in the boundary layer proves to be larger than the critical Rayleigh numbers for the transition from soft turbulence to hard turbulence in RB convection, i.e. $\mathrm{Ra}^* > \mathrm{Ra}_{c3}$.

In what follows, we will assume that each regime of heat transfer in the entire volume V of heat-generating fluid is a combination of convection regimes that take place in region V_+ and in the boundary layer. Hence, in view of the definition of the number Nu, we have

$$\mathrm{Nu}_{\mathrm{up}} \propto \frac{H}{H_+}\,\mathrm{Ra}_+^{\beta_{\mathrm{RB}}} = \left(\frac{H}{H_+}\right)^{1-3\beta_{\mathrm{RB}}} \mathrm{Ra}^{\beta_{\mathrm{RB}}}\,, \tag{3.10}$$

$$\mathrm{Nu}_{\mathrm{dn}} \propto \mathrm{Ra}^{\beta_{\mathrm{bl}}}\,. \tag{3.11}$$

Since the interface between V_+ and V_- corresponds to the maximum of the average temperature, the difference between H_+ and H_- is closely related to the difference between $\mathrm{Nu}_{\mathrm{up}}$ and $\mathrm{Nu}_{\mathrm{dn}}$. If we take into account the inequalities

$$|\beta_{\mathrm{RB}} - \beta_{\mathrm{bl}}| \ll \beta_{\mathrm{bl}}\,, \qquad 1 - 3\beta_{\mathrm{RB}} \ll 1 \tag{3.12}$$

and the fact that at modified Rayleigh numbers $\mathrm{Ra_i} \leqslant 10^{13} - 10^{14}$ the case of $\beta_{\mathrm{RB}} > \beta_{\mathrm{bl}}$ and the opposite one are realized alternately, we can assume that within this range $H_+ \approx H/2$ and, accordingly, set $\mathrm{Ra}_+ \approx (1/8)\mathrm{Ra}$. In this range of $\mathrm{Ra_i}$ we have, in view of (3.3) and (3.5), the following relationship:

$$\beta = \frac{\beta_{\mathrm{up}} + \beta_{\mathrm{dn}}}{2} \pm \frac{|\beta_{\mathrm{up}} - \beta_{\mathrm{dn}}|}{2}\,. \tag{3.13}$$

Relationships (3.10), (3.11), and (3.13) and the above information about the characteristics of heat transfer in a fluid without internal heat sources enable us to specify four basic regimes, which differ in the type of convection in V_+ and the boundary layer and, accordingly, in the exponents β, ε, and γ_i given by (3.5).

(i) $\mathrm{Ra_i^{(1)}} < \mathrm{Ra_i} < \mathrm{Ra_i^{(2)}}$:
laminar convection in V_+ and the boundary layer,

$$\beta = 0.25\,, \quad \varepsilon = 0.8\,, \quad \gamma_{\mathrm{up}} = \gamma_{\mathrm{dn}} = 0.2\,; \tag{3.14}$$

(ii) $\mathrm{Ra_i^{(2)}} < \mathrm{Ra_i} < \mathrm{Ra_i^{(3)}}$:
soft turbulence in V_+ and laminar flow in the boundary layer,

$$\beta = 0.290 \pm 0.040\,, \quad \varepsilon = 0.775 \pm 0.025\,,$$

$$\gamma_{\mathrm{up}} = 0.263 \pm 0.008\,, \quad \gamma_{\mathrm{dn}} = 0.195 \pm 0.005\,; \tag{3.15}$$

(iii) $\mathrm{Ra_i^{(3)}} < \mathrm{Ra_i} < \mathrm{Ra_i^{(4)}}$:
hard turbulence in V_+ and laminar flow in the boundary layer,

$$\beta = 0.270 \pm 0.020\,, \quad \varepsilon = 0.790 \pm 0.030\,,$$

$$\gamma_{\mathrm{up}} = 0.225 \pm 0.004\,, \quad \gamma_{\mathrm{dn}} = 0.197 \pm 0.003\,; \tag{3.16}$$

(iv) $\mathrm{Ra_i^{(4)}} < \mathrm{Ra_i} < 10^2\mathrm{Ra_i^{(4)}}$:
hard turbulence in V_+ and a combination of laminar and turbulent flows in the boundary layer,

$$\beta = 0.31 \pm 0.025\,, \quad \varepsilon = 0.765 \pm 0.015\,,$$

$$\gamma_{\mathrm{up}} = 0.218 \pm 0.004\,, \quad \gamma_{\mathrm{dn}} = 0.255 \pm 0.005 \tag{3.17}$$

(the exponents given for regime (iv) correspond to the endpoint of the interval of Rayleigh numbers for this regime).

In accordance with the above characteristics of heat transfer in a fluid without internal heat sources and in view of (3.13), (3.5), and (3.6), we can define the boundaries between regimes (i)–(iv) as follows:

$$\mathrm{Ra_i^{(1)}} \simeq 10^5\,, \quad \mathrm{Ra_i^{(2)}} \simeq 15(\mathrm{Ra_{c2}})^{1.25}\,,$$

$$\mathrm{Ra_i^{(3)}} \simeq 15(\mathrm{Ra_{c3}})^{1.29}\,, \quad \mathrm{Ra_i^{(4)}} \simeq 15(\mathrm{Ra}^*)^{1.27}\,. \tag{3.18}$$

Here, $\mathrm{Ra_i^{(2)}}$ and $\mathrm{Ra_i^{(3)}}$ depend on the aspect ratio A for V_+ and $\mathrm{Ra_i^{(4)}}$ on the Prandtl number. At sufficiently high aspect ratios A regime (ii) may not occur, in which case regime (i) is directly followed by regime (iii). As noted above, there is some ambiguity in the dependence of the critical value Ra^* on the Prandtl number Pr. Accordingly, this ambiguity affects $\mathrm{Ra_i^{(4)}}$. To illustrate this point, we note that for a fluid with thermal–hydrodynamic characteristics corresponding to water, $\mathrm{Ra_i^{(4)}} \simeq 2.5 \times 10^{13}$ [53].

The $\mathrm{Ra_i}$ interval from 10^{13} to 10^{17} is of most interest from the viewpoint of reactor safety. Regime (iv) falls within this interval, where turbulent flows replace laminar flows in the boundary layer. At $\mathrm{Ra_i} > 10^2\mathrm{Ra_i^{(4)}}$, the turbulent part of the boundary layer becomes predominant. If we take into account the numerical factors in the dependences Nu(Ra) for the laminar and turbulent boundary layers in a fluid without internal heat sources [13, 49], we can approximately represent the dependence $\mathrm{Nu}_{\mathrm{dn}}$ (Ra) in regime (iv) for a heat-generating fluid as follows:

$$\mathrm{Nu}_{\mathrm{dn}} \approx 0.68(\mathrm{Ra}^*)^{1/4} + 0.15\left[\mathrm{Ra}^{1/3} - (\mathrm{Ra}^*)^{1/3}\right]. \tag{3.19}$$

The flow-regime transition in the boundary layer makes the dependence $\mathrm{Nu}_{\mathrm{dn}}$ (Ra) much stronger. As before, we describe this dependence by a formula like (3.5), to obtain the exponent γ_{dn} as the logarithmic derivative of (3.19). This exponent will be a function of $\mathrm{Ra_i}$. We define the averaged γ_{dn} as follows:

$$\bar{\gamma}_{\mathrm{dn}} = \frac{\Delta \ln \mathrm{Nu}_{\mathrm{dn}}}{\Delta \ln \mathrm{Ra_i}}\,, \tag{3.20}$$

where $\Delta \ln \mathrm{Nu}_{\mathrm{dn}}$ is the variation of $\ln \mathrm{Nu}_{\mathrm{dn}}$ over the averaging interval from $\mathrm{Ra_i^{(4)}}$ to $\mathrm{Ra_i^{(4)}} \exp[\Delta \ln \mathrm{Ra_i}]$. We assume that $\mathrm{Ra_i^{(4)}} = 2.5 \times 10^{13}$ corresponds to a fluid with thermal–hydrodynamic properties typical of water and that $\Delta \ln \mathrm{Ra_i} = \ln 10^2$; and then, in view of (3.19), we use (3.20) to estimate $\bar{\gamma}_{\mathrm{dn}}$ on the interval where the flow regime in the boundary layer changes:

$$\bar{\gamma}_{\mathrm{dn}} \approx 0.36\,. \tag{3.21}$$

3.4 Asymptotic regime

The interface between V_+ and V_- is determined by the position of the maximum of the average temperature of the fluid in volume V. Therefore, as $\mathrm{Ra_i}$ increases, at $\beta_{\mathrm{up}} \neq \beta_{\mathrm{dn}}$, this interface moves ensuring a minimum increase in the temperature difference ΔT. Up $\mathrm{Ra_i} = \mathrm{Ra_i^{(4)}}$, we have $\beta_{\mathrm{up}} \geqslant \beta_{\mathrm{dn}}$, so that the interface gradually moves downward as $\mathrm{Ra_i}$ increases. After the transition to the turbulent regime in the boundary layer is completed, β_{dn} becomes larger than β_{up}, and a further increase in $\mathrm{Ra_i}$ does not change this relationship between the two exponents. This implies that, at this stage of increase of $\mathrm{Ra_i}$, the interface between regions V_+ and V_- monotonically moves upward. This finally leads to an asymptotic situation in which $V_+ \ll V$ and $H_+ \ll H$ and the heat generated in V_+ leaves this volume through the upper boundary $\mathrm{S_{up}}$ almost completely. In these conditions, relationships (3.5)–(37), (3.10), (3.11), and the relationship that follows from the condition for energy balance in V_+ yield

$$\beta = \frac{1}{3}\,, \quad \varepsilon = \frac{3}{4}\,, \quad \gamma_{\mathrm{dn}} = \frac{1}{4}\,, \quad \gamma_{\mathrm{up}} = \frac{7}{32} \approx 0.219\,. \qquad (3.22)$$

These exponents specify the characteristics of the asymptotic regime of heat transfer in a heat-generating fluid. This regime takes place at

$$\mathrm{Ra_i^{-1/32}} \ll 1\,. \qquad (3.23)$$

Note that the asymptotic behavior of the heat transfer for a plane horizontal fluid layer with internal heat sources was studied by Cheung [54], who assumed that, at asymptotically large Rayleigh numbers, a soft-turbulence convection regime occurs (hard turbulence was discovered later) and found $\beta_{\mathrm{up}} = 1/4$ for the heat transfer through the upper boundary.

3.5 Comparison with experiment

We begin with an important remark concerning the aspect ratio for volume V_+ containing a heat-generating fluid. As noted above, at moderate Rayleigh numbers and provided the entire boundary is cooled, we have the estimate $H_+ \sim H/2$. On the other hand, in all known experiments the ratio of the horizontal size of the model volume to its height is about two or more. Hence the aspect ratio A than for V_+ is no less four. At the same time, the lower limit of the interval of Rayleigh numbers in experiments was no less than 10^4. Comparison of these facts leads to the following conclusion. Over the entire range of Rayleigh numbers corresponding to the known experiments on heat transfer in fluids with internal heat sources, according to Wu and Libchaber's results [48], hard turbulence occurs in V_+. This means that regimes (i) and (ii), as classified in Section 3.3, did not occur in these experiments.

We start our comparison between theoretical and experimental results with the experiment of Kulacki and Emara [17], since it is most suitable for testing the theory. We recall that these researchers studied heat transfer through the upper boundary of a plane horizontal layer of fluid with internal heat sources and a thermally insulated lower boundary. The aspect ratio of the model volume ($A = D/H$) varied from 2 to 40, and the modified Rayleigh number ranged from 2×10^4 to 4×10^{12} [see (2.3)]. Since small values of $\mathrm{Ra_i}$ corresponded to large values of the aspect ratio, the above remark implies that the entire range of Rayleigh numbers in Kulacki and Emara's studies [17] corresponded to the hard turbulence regime for RB convection. Hence we should substitute $\beta_{\mathrm{RB}} = 2/7$ into the formula for the exponent that determines the heat transfer through the upper boundary in the given experiment, which, according to (3.7), has the form

$$\gamma_{\mathrm{up}} = \frac{\beta_{\mathrm{RB}}}{1 + \beta_{\mathrm{RB}}}\,. \qquad (3.24)$$

Thus, we obtain $\beta_{\mathrm{up}}^{\mathrm{theor}} \approx 0.222$. This result is in good agreement with the experimental value of this exponent [9] [see (2.3)], $\beta_{\mathrm{up}}^{\mathrm{exp}} = 0.227$.

It goes without saying that such close results can also be interpreted as experimental evidence for the analogy between the mechanisms of heat transfer in V_+, which belongs to the volume containing the heat-generating fluid, and RB convection.

Two other experiments described, respectively, in Refs [16, 19] and Ref. [21], were carried with isothermal boundary conditions and a modified Rayleigh number of about 10^{13}, so that, by the classification of Section 3.3, these experiments belong to regime (iii). In Table 1 we compare the experimental and theoretical values of the exponents that refer to the given experiments.

Table 1. Comparison of theoretical results and the results of experiments on heat transfer for totally isothermal boundary conditions and moderate modified Rayleigh numbers.

γ_{up}		γ_{dn}	
Experiment	Theory	Experiment	Theory
0.23 [16, 19]	0.225 ± 0.004	0.18 [16, 19]	0.197 ± 0.003
0.233 [21]		0.19 [21]	

In their experiments with the ACOPO facility, Theofanous and Liu [29] found that, as the Rayleigh number was increased, the rate of heat transfer through the lower boundary grew substantially, which was described by a power-law dependence with an exponent $\gamma_{\mathrm{dn}} = 0.35$. Note that the explored range $3 \times 10^{13} < \mathrm{Ra_i} < 7 \times 10^{14}$ may correspond to heat-transfer regime (iv), with a change from laminar to turbulent flow in the boundary layer on S_{dn}. If this is the case, the theoretical estimate (3.21), $\gamma_{\mathrm{dn}}^{\mathrm{theor}} \simeq 0.36$, completely agrees with the results of Theofanous and Liu [29]. We also note that the change of regime in the boundary layer at the vertical section of the boundary in the same range of $\mathrm{Ra_i}$ values was also recorded by Alvarez et al. [22] in their experiment with the BAFOND facility.

Particular attention should also be given to the experiment by Bonnet and Seiler [28], who used the BALI facility and extremely high modified Rayleigh numbers, $10^{15} < \mathrm{Ra_i} < 10^{17}$. They obtained exponents that correspond to $\gamma_{\mathrm{up}} = 0.216$ and $\gamma_{\mathrm{dn}} = 0.25$. Actually, these values agree almost perfectly with the theoretical exponents for the asymptotic heat-transfer regime [formula (3.22)];

$$\gamma_{\mathrm{up}}^{\mathrm{theor}} \simeq 0.219\,, \quad \gamma_{\mathrm{dn}}^{\mathrm{theor}} = 0.25\,.$$

Theofanous et al. [30] used the ACOPO facility and obtained empirical relationships for heat transfer through the upper and lower boundaries with exponents that differ from those of Bonnet and Seiler [28]. However, in both cases the relation between the exponents is characteristic of extremely high rates of heat generation:

$$\gamma_{\mathrm{dn}} > \gamma_{\mathrm{up}}\,, \quad \mathrm{Ra_i} > 10^{14}\,, \qquad (3.25)$$

which confirms the presence of a tendency toward the asymptotic regime with heat removal occurring predominantly through the lower boundary.

To summarize, we can note that agreement between theory and experiment in relation to the integral characteristics of heat transfer is quite satisfactory.

4. Regularities of the local-heat-flux distribution

4.1 Statement of the problem

In the previous section we obtained analytical estimates for heat-transfer characteristics averaged separately over the upper and the lower section of the boundary. However, to solve problems related to reactor safety, one must know in greater detail the distribution of heat transfer from a fluid with internal heat sources. This, in particular, refers to the lower part of the boundary, where special conditions for the external cooling by boiling water are present [55].

In this section we consider the regularities of the heat-flux distribution and the characteristics of convection in the lower part of a volume containing a fluid with internal heat sources.

We assume that, near the lowest point (the pole), the curvature radius R of the boundary is finite. We also assume that the height H of the fluid volume is comparable to R. The position of a point at the boundary is specified by the angle θ between the normal to the boundary and the vertical axis (so that $\theta = 0$ at the pole). We denote the coordinate measured from the pole upward by z. What we are interested in are the characteristics of convection in the region where $\theta \ll 1$ and $z \ll H$. The geometry of the lower part of the volume is schematically depicted in Fig. 2.

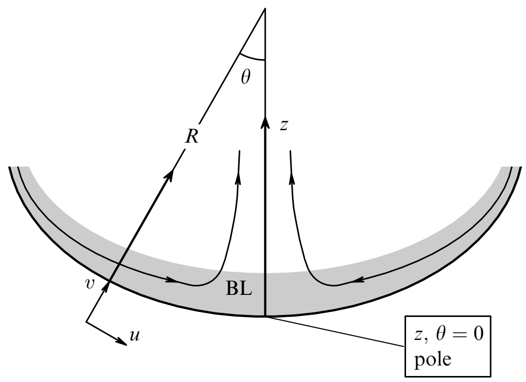

Figure 2. Geometry of the lower part of the cavity filled with a fluid: θ is the polar angle, z is the vertical coordinate measured from the lowest point (the pole) upward, R is the curvature radius of the boundary at the pole ($\theta = 0$), and u and v are the longitudinal and transverse components of the velocity in the boundary layer, respectively.

Heat transfer through the lower boundary is determined by the characteristics of the boundary layer that forms there. For angles $\theta \sim 1$, this layer, as noted in Section 3, is similar to the well-studied natural-convection boundary layer at a vertical wall in a fluid without internal heat sources [13]. As the pole is approached ($\theta \ll 1$), the properties of the boundary layer change dramatically. Here the boundary layer becomes convergent, as evident from geometric conditions. This fact leads to the important condition that the longitudinal component of the boundary-layer velocity must vanish at the pole:

$$u(\theta = 0) = 0\,. \tag{4.1}$$

The condition means that, for $\theta \ll 1$, the boundary layer decelerates rather then accelerates, in contrast to the case of $\theta \sim 1$. Moreover, in contrast to the region $\theta \sim 1$, where the boundary layer 'sucks' the fluid from the bulk of the volume, at $\theta \ll 1$ the layer returns the fluid to the bulk. Another important property of the boundary layer at $\theta \ll 1$ is that the buoyancy in the longitudinal direction is weakened.

The flow velocity and the temperature of the fluid in the bulk of the volume (outside the boundary layer) are, due to condition (4.1), strongly z-dependent if $z \ll H$. This fact, in turn, has a strong reverse effect on the characteristics of the boundary layer itself. Hence problems concerning the boundary layer and the flow and temperature distributions outside the boundary layer should be solved in conjunction with the matching conditions at the free surface of the boundary layer (i.e. the surface facing the bulk of the fluid). These are continuity conditions for the temperature and the normal component of the velocity:

$$T \approx T_{\mathrm{b}}\,, \qquad y \approx \delta\,, \tag{4.2}$$

$$v \approx v_{\mathrm{b}}\,, \qquad y \approx \delta\,, \tag{4.3}$$

where T and T_{b} are the temperatures in the boundary layer and bulk, respectively, v and v_{b} are the components of the flow velocity normal to the boundary in the boundary layer and in the bulk, u is the longitudinal component of the velocity, y is the coordinate measured from the boundary and normal to it (see Fig. 2), and δ is the thickness of the boundary layer. Note that, since $\theta \ll 1$, the component v_{b} is at the same time the vertical component of the velocity in the bulk of the fluid.

In the next section we discuss the relationships between the boundary-layer characteristics and the distributions of temperature and flow velocity in the bulk of the volume. We examine the cases of laminar and turbulent boundary layers separately.

4.2 Relationships for a convergent boundary layer

Laminar boundary layer. In the region where the polar angle satisfies the condition

$$\frac{\delta}{R} \ll \theta^2 \ll 1\,, \tag{4.4}$$

the system of equations expressing the conservation of mass, longitudinal component of momentum, and energy for the fluid in a laminar boundary layer assumes the form

$$-\frac{1}{R\theta}\frac{\partial}{\partial\theta}(\theta u) + \frac{\partial v}{\partial y} = 0\,, \tag{4.5}$$

$$-\frac{1}{R\theta}\frac{\partial}{\partial\theta}(\theta u^2) + \frac{\partial}{\partial y}(vu) - \nu\frac{\partial^2 u}{\partial y^2} = g\alpha(T_{\mathrm{b}} - T)\theta\,, \tag{4.6}$$

$$-\frac{1}{R\theta}\frac{\partial}{\partial\theta}(\theta u T) + \frac{\partial}{\partial y}(vT) = \chi\frac{\partial^2 T}{\partial y^2}\,. \tag{4.7}$$

In deriving the system of equations (4.5)–(4.7), pressure was eliminated by employing the equation of balance for the transverse component of the boundary-layer momentum. The left inequality in (4.4) made it possible, in particular, to neglect the contribution of bulk heat emission in equation (4.7) and the inertia force due to the transformation to the curvilinear coordinate system in equation (4.6).

For our further discussion, we need to determine the shape of the transverse temperature profile in the boundary layer. In an ordinary natural-convection boundary layer near the vertical wall, if the temperature of the fluid is coordinate-independent, the temperature profile in the bulk volume is monotonic [13]. A different situation arises if a thermal inhomogeneity is present due to a stable stratification in the bulk. Since the temperature at the outer side of the boundary layer must coincide with the ambient temperature [see equation (4.2)], then, as we move downstream, the temperature inside the boundary layer becomes higher than at the outer side due to convective transport from the upper, hotter sections. As a result, the buoyancy force is directed oppositely to the longitudinal velocity in the boundary layer, so that the fluid in the boundary layer slows down and, ultimately, the boundary condition (4.1) is met. Since the temperature distribution in the bulk is formed by the backflow from the boundary layer, the maximum excess of temperature inside the boundary layer over the ambient temperature should be of the same order of magnitude as the latter is:

$$\max(T - T_{\mathrm{b}}) \sim T_{\mathrm{b}} \,. \tag{4.8}$$

The temperature profile inside a convergent boundary layer is depicted schematically in Fig. 3.

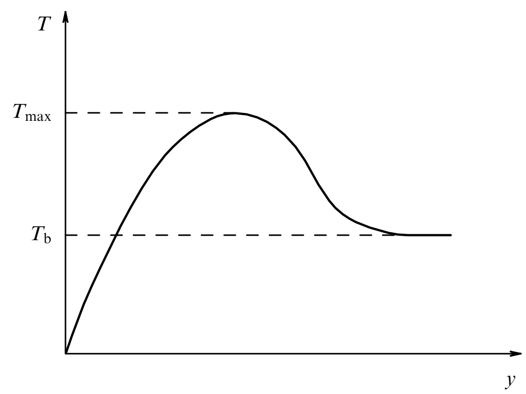

Figure 3. Temperature profile for a convergent boundary layer: T is the temperature, y is the coordinate normal to the boundary, $T_{\max}$ is the maximum temperature inside the boundary layer, and T_{b} is the temperature in the bulk region adjacent to the boundary layer.

Note that a nonmonotonic temperature profile in the boundary layer near the vertical wall of a stratified fluid was reported in [56] based on numerical simulations and experiments.

Now we derive the relationships between the characteristics of the boundary layer and those of the bulk. Combining equations (4.5)–(4.7), the estimate (4.8), and the matching conditions (4.2) and (4.3) yields the following relationships:

$$\frac{u}{R\theta} \sim \frac{v_{\mathrm{b}}}{\delta} \,, \tag{4.9}$$

$$\left(\frac{u}{R\theta}\right)^2 \sim \frac{g\alpha T_{\mathrm{b}}}{R} \,, \tag{4.10}$$

$$v_{\mathrm{b}} \sim \frac{\chi}{\delta} \,. \tag{4.11}$$

Another relationship follows from the very definition of the heat flux at the boundary:

$$q \sim \frac{\lambda T_{\mathrm{b}}}{\delta} \,. \tag{4.12}$$

Eliminating the velocity u from (4.9)–(4.11) and using (4.12), we arrive at important formulas that link the vertical component of velocity and the heat-flux density to the bulk temperature:

$$v_{\mathrm{b}} \propto \left(\frac{\chi^2 g\alpha T_{\mathrm{b}}}{R}\right)^{1/4} , \tag{4.13}$$

$$q \propto \lambda \left(\frac{g\alpha T_{\mathrm{b}}^5}{\chi^2 R}\right)^{1/4} . \tag{4.14}$$

We now dwell on the case of very small polar angles,

$$\theta^2 \ll \frac{\delta}{R} \,. \tag{4.15}$$

The mass balance condition (4.5) in this region yields the following estimate:

$$u \sim u_* \frac{\theta}{\theta_*} \,, \tag{4.16}$$

where u_* is the value of u at $\theta = \theta_*$, with the angle θ_* defined as

$$\theta_*^2 \sim \frac{\delta(\theta_*)}{R} \,. \tag{4.17}$$

In view of (4.16), it follows from the balance condition for the longitudinal component of momentum that, for angles defined by (4.15), the temperature in the boundary layer is polar-angle-independent. Then, in accordance with the estimate (4.16), we can neglect the first term in the energy balance equation for this range of angles. At the same time, we must restore the term responsible for volumetric heat generation in this equation. This results in the equation

$$v\frac{\partial T}{\partial y} = \chi \frac{\partial^2 T}{\partial y^2} + \frac{Q}{\rho C} \,, \tag{4.18}$$

where C is the specific heat of the fluid. This implies that, for very small polar angles $\theta \ll \theta_*$, the thickness of the boundary layer and the temperature do not depend on the polar angle and the estimates for these quantities are

$$\delta \sim \delta_* \sim \frac{\chi}{v_*} \,, \qquad T \sim T(\theta_*) \sim \frac{Q\delta_*^2}{\lambda} \,, \tag{4.19}$$

where v_* is the velocity v at $\theta \sim \theta_*$. Finally, it follows from (4.19) and (4.12) that for such angles ($\theta \ll \theta_*$) the heat flux density at the boundary is also virtually constant. At the pole ($\theta = 0$) this flux density is minimal, and its value can be estimated as

$$q_{\min} \sim q_* \equiv q(\theta_*) \sim \langle q \rangle \theta_*^2 \,, \tag{4.20}$$

where $\langle q \rangle \sim QR$ is the heat flux averaged over the entire boundary.

Turbulent boundary layer. In order to derive relationships for a turbulent boundary layer similar to those for a laminar boundary layer, we note that most part of the temperature drop corresponds to the viscous conductive sublayer, where the mass, momentum, and energy balance conditions are local. Hence the estimate that relates the heat-flux density at the wall to the ambient temperature for a convergent turbulent boundary layer coincides with the estimate for a turbulent boundary layer at the vertical wall in the case of an isothermal ambient [49]:

$$q \propto \lambda \left(\frac{g\alpha T_{\mathrm{b}}^4}{\chi^2} \right)^{1/3} . \tag{4.21}$$

To relate the vertical component of velocity v_{b} to the temperature T_{b} in the bulk volume, we turn to the turbulent core of the boundary layer, where viscosity and heat conductivity are insignificant. In this region the relationship between the longitudinal component of velocity averaged over the turbulent pulsations (for which we retain the notation u) and the vertical component of velocity in the bulk volume coincides, according to the mass balance condition and the matching condition (4.3), with the estimate (4.9). The momentum and energy balance conditions for the turbulent core lead to the following estimates:

$$\left(\frac{u}{R\theta} \right)^2 \sim \frac{g\alpha \Delta T}{R} , \tag{4.22}$$

$$v'^2 \sim g\alpha T' \delta , \tag{4.23}$$

$$q \sim \rho C v' T' , \tag{4.24}$$

where ΔT is the characteristic averaged excess of temperature in the turbulent core over the temperature of the adjacent regions of the bulk volume, and v' and T' are the characteristic values of the turbulent pulsations of velocity and temperature, respectively. Since $v' \sim v_{\mathrm{b}}$ and $T' \sim \Delta T$, we obtain the following estimates from (4.9) and (4.22)–(4.24):

$$\left(\frac{u\delta}{R\theta} \right)^3 \sim g\alpha \frac{q}{\rho C} \delta , \tag{4.25}$$

$$u^3 \sim g\alpha \frac{q}{\rho C} \frac{R^2 \theta^3}{\delta} , \tag{4.26}$$

$$v_{\mathrm{b}} \sim \left(\chi R^3 (g\alpha T_{\mathrm{b}})^4 \right)^{1/9} , \tag{4.27}$$

$$q \sim \frac{\lambda}{g\alpha\chi R} v_{\mathrm{b}}^3 . \tag{4.28}$$

4.3 Bulk temperature and flow velocity

In the bulk volume (outside the boundary layer), since viscosity and heat conductivity are insignificant there, the momentum and energy balance conditions become

$$(\mathbf{v}_{\mathrm{b}} \operatorname{grad}) \mathbf{v}_{\mathrm{b}} = -\frac{\operatorname{grad} p}{\rho} + g\alpha T_{\mathrm{b}} \mathbf{n} , \tag{4.29}$$

$$(\mathbf{v}_{\mathrm{b}} \operatorname{grad}) T_{\mathrm{b}} = \frac{Q}{\rho C} . \tag{4.30}$$

Here, $\mathbf{v}_{\mathrm{b}} = \mathbf{v}_{\mathrm{h}} + v_{\mathrm{v}} \mathbf{n}$ is the velocity vector in the bulk, $\mathbf{n}$ is the unit vector along the z axis, and v_{v} and v_{h} are the vertical and horizontal components of velocity.

Compared to the flow in the boundary layer, the bulk flow is much slower. In view of this, the buoyancy force resulting from the inhomogeneity of the temperature distribution is almost completely balanced by the pressure gradient. This means that a nearly hydrostatic situation emerges in this region, in which case, as is known [7], the temperature depends on only one variable, the z coordinate, and the stratification is stable if the temperature gradient is directed along the z axis. Let us estimate the corrections to the stratified temperature distribution due to the presence og a slow motion.

We denote the characteristic pressure variation over the horizontal cross section of the bulk volume at a fixed z coordinate by Δp_{h}. In view of the horizontal component of equation (4.29), we have

$$\Delta p_{\mathrm{h}} \sim \rho v_{\mathrm{h}}^2 .$$

With the use of the vertical component of equation (4.29), we obtain the characteristic temperature variation in the same cross section:

$$(\Delta T_{\mathrm{b}})_{\mathrm{h}} \sim \frac{v_{\mathrm{h}}^2}{g\alpha z} . \tag{4.31}$$

If we allow for the fact that the linear size of the horizontal cross section in the case of $z \ll R$ considered here is of order $\sqrt{Rz}$, the mass balance equation for the bulk volume leads to the following relationship between the horizontal (v_{h}) and vertical (v_{v}) components of velocity:

$$v_{\mathrm{h}}^2 \sim \frac{R}{z} v_{\mathrm{v}}^2 . \tag{4.32}$$

We substitute (4.32) into (4.31) and use formulas (4.13) and (4.11) to obtain the estimate

$$(\Delta T_{\mathrm{b}})_{\mathrm{h}} \sim \left(\frac{\delta}{z} \right)^2 T_{\mathrm{b}} . \tag{4.33}$$

This implies that for values of height z much larger than the thickness of the boundary layer δ, the corrections due to the dependence of temperature on the horizontal coordinates are small and

$$T_{\mathrm{b}} \simeq T_{\mathrm{b}}(z) . \tag{4.34}$$

Therefore, br virtue of (4.3), we find that a similar statement holds for the vertical component of velocity under the same condition $z \gg \delta$:

$$v_{\mathrm{v}} \approx v_{\mathrm{v}}(z) . \tag{4.35}$$

If we take into account (4.34) and (4.35), equation (4.30) becomes

$$v_{\mathrm{v}} \frac{dT_{\mathrm{b}}}{dz} = \frac{Q}{\rho C} . \tag{4.36}$$

In particular, this implies that in the bulk region adjacent to the boundary layer, where, for $\theta \ll 1$, we have the approximation $z \simeq R\theta^2/2$, the following estimate is valid:

$$T_{\mathrm{b}} \sim \frac{Q}{\rho C} \frac{R\theta^2}{2v_{\mathrm{v}}} . \tag{4.37}$$

4.4 Limiting relationships

In the region of polar angles specified by inequality (4.4), equations (4.5)–(4.7) do not contain any scale for the polar angle θ. Hence the dependences of the parameters of the fluid on the angle θ and the height z should be of power-law form. We define the exponents a, b, f, and d through the following relationships:

$$q \propto \theta^a\,, \quad T_\mathrm{b} \propto \left(\frac{z}{R}\right)^b, \quad u \propto \theta^f\,, \quad \delta \propto \theta^d\,. \tag{4.38}$$

As earlier, we discuss the cases of laminar and turbulent flow regimes in the boundary layer separately.

Laminar boundary layer. The substitution of the definitions (4.38) into equations (4.9)–(4.12) and (4.37) and the elimination of v_v, yield the following system of linear algebraic equations for the exponents:

$$f = b + 1\,, \quad f = 1 - 2d\,, \quad 2b + f + d = 3\,, \quad a = 2b - d\,. \tag{4.39}$$

The solution of this system leads to the following result:

$$a = 2\,, \quad b = \frac{4}{5}\,, \quad c = \frac{9}{5}\,, \quad d = -\frac{2}{5}\,. \tag{4.40}$$

Turbulent boundary layer. By analogy to the preceding case, we substitute the definitions (4.38) into equations (4.21), (4.25), (4.26), and (4.37) to obtain

$$\begin{gathered} 3f + 2d - a = 3\,, \quad 3f + d - a = 3\,, \\ 2b + f + d = 3\,, \quad a = \frac{8b}{3}\,. \end{gathered} \tag{4.41}$$

The solution of this system yields

$$a = \frac{24}{13}\,, \quad b = \frac{9}{13}\,, \quad c = \frac{21}{13}\,, \quad d = 0\,. \tag{4.42}$$

Equations (4.38), (4.40), and (4.42) describe the behavior of the heat flux at the boundary and the distribution of thermal–hydraulic characteristics in the lower part of the volume containing a fluid with internal heat sources. Note that the exponent b responsible for the temperature distribution in the bulk volume, is smaller than unity. Hence, according to (4.38), we have the inequality

$$\frac{\partial^2 T_\mathrm{b}}{\partial z^2} < 0\,. \tag{4.43}$$

4.5 Discussion and comparison with experiment

For small polar angles, $\theta \ll 1$, the heat-flux density at the boundary decreases very rapidly with the decrease of the angle, due to the thickening of the boundary layer and to the temperature stratification in the bulk. As a result [see equation (3.43)], the pattern of horizontal isotherms becomes denser as we approach the lower boundary of the bulk volume. The asymptotic behavior of the heat flux at the boundary and the bulk temperature distribution depend on the flow regime in the boundary layer. For a laminar boundary layer, the asymptotic dependences for $\theta_* \ll \theta \ll 1$ and $\delta \ll z \ll R$ are given, according to (4.38) and (4.40), by the expressions

$$q \propto \theta^2\,, \quad T_\mathrm{b} \propto \left(\frac{z}{H}\right)^{4/5}. \tag{4.44}$$

At $\theta \sim \theta_*$, where the angle $\theta_* \ll 1$ is defined by (4.17), the decrease of the heat-flux density with the decrease of the polar angle slows down and becomes almost constant for $\theta \ll \theta_*$, reaching a minimum at the pole ($\theta = 0$).

The asymptotic dependences for turbulent flow regimes in the boundary layer are, according to (4.38) and (4.42), as follows:

$$q \propto \theta^{24/13}\,, \quad T_\mathrm{b} \propto \left(\frac{z}{H}\right)^{9/13}. \tag{4.45}$$

The turbulent flow regime in a convergent boundary layer is possible if this regime develops at an earlier (upstream) stage at angles $\theta \sim 1$. In this case, according to (4.38) and (4.42), the Reynolds number for angles $\theta \ll 1$ varies according to the law

$$\mathrm{Re} \equiv \frac{u\delta}{v} \propto \theta^{21/13}\,. \tag{4.46}$$

If the threshold of the laminar–turbulent transition in the boundary layer is not exceeded very strongly, the Reynolds number rapidly falls below the critical value with the decreases of the polar angle, and we return to the asymptotic dependences (4.44).

We estimate the minimum heat-flux density attained at $\theta = 0$ and the threshold angle θ_* below which the angular dependence of the heat flux-density weakens substantially. According to (4.38) and (4.40), the angular dependence of the boundary layer thickness is determined by the formula

$$\delta(\theta) = \delta_0 \theta^{-2/5}\,, \tag{4.47}$$

where δ_0 is a quantity of the order of the boundary-layer thickness at $\theta \sim 1$. The substitution of (4.47) into (4.17) yields the sought estimate for θ_*:

$$\theta_* \sim \left(\frac{\delta_0}{R}\right)^{5/12}. \tag{4.48}$$

In accordance with (4.12) and the results of the preceding section, the dependence of δ_0 on the modified Rayleigh number is given by the estimate $\delta_0/R \sim \mathrm{Ra}_\mathrm{i}^{-\gamma_\mathrm{dn}}$, where $\gamma_\mathrm{dn} \simeq 0.2$. This result with equations (4.48), (4.17), and (4.20) taken into account gives an estimate for the ratio of the minimum to the average heat-flux density and for the angle θ_*:

$$\frac{q_\mathrm{min}}{\langle q \rangle} \sim \mathrm{Ra}_\mathrm{i}^{-1/6}\,, \quad \theta_* \sim \mathrm{Ra}_\mathrm{i}^{-1/12}\,. \tag{4.49}$$

To conclude this section, we compare the above results with experiment. First, we note that all experimental data demonstrate a rapid decrease in the heat-flux density with the decrease of the polar angle for $\theta \ll 1$. They also point to the presence of a temperature stratification in the bulk of the volume for $z \ll H$. The theoretical results described by equations (4.44) and (4.49) and the experimental data obtained by Frantz and Dhir [24], Kymäläinen et al. [25], and Bonnet and Seiler [28] are listed in Table 2. We see that there is qualitative agreement between theory and experiment in what concerns the angular dependence of the heat-flux density and the ratio of the minimum to the average value of this density. At the same time, a more detailed comparison would require higher accuracy and spatial resolution in measurements of the heat-flux density.

Jahn [19] used optical methods to record the temperature distribution within the volume of a fluid with internal heat sources. Figure 4 depicts a typical hologram, taken from Ref.

Table 2. Heat-flux distribution at the boundary: comparison of theory and experiment.

	Experiment	Theory
UCLA [24], $\mathrm{Ra_i} = (3-8) \times 10^{13}$	$q_{\min}/\langle q\rangle \simeq 0{,}1$ $q\,\theta/\langle q\rangle = a + b\theta^2$	$q_{\min}/\langle q\rangle \sim 10^{-2}$ $q(\theta)/\langle q\rangle \approx a + b\theta^2$
COPO [25], $\mathrm{Ra_i} \sim 10^{14}-10^{15}$	$q_{\min}/\langle q\rangle \simeq 0$	$q_{\min}/\langle q\rangle \simeq 10^{-3}$
BALI [28], $\mathrm{Ra_i} \sim 10^{15}-10^{17}$	$q_{\min}/\langle q\rangle < 10^{-2}$	$q_{\min}/\langle q\rangle \sim (1-5) \times 10^{-3}$

[19], that describes the pattern of isotherms. One can clearly see the temperature stratification and an increase in the density of horizontal isotherms as the lower boundary is approached. Such behavior agrees with the theoretical formula (4.43). In Fig. 5, we quantitatively compare the theoretical results with the results of Jahn's experiment [19] for the temperature distribution within the bulk volume at a heat-generation rate in the fluid corresponding to $\mathrm{Ra_i} = 1.04 \times 10^8$. The theoretical dependence of the reduced temperature on the dimensionless reduced height was specified, in accordance with formula (4.44), by the relationship $T_b \propto z^{4/5}$, while the experimental points were obtained by numerically processing the hologram in Fig. 4.

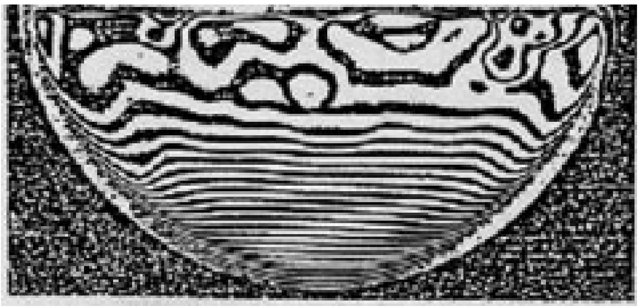

Figure 4. Typical hologram from Ref. [19] describing the distribution of isotherms in the main volume: the dark lines correspond to isotherms.

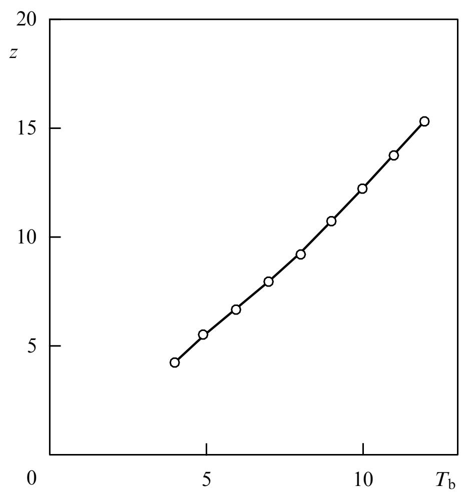

Figure 5. Temperature distribution in the main volume: comparison of theoretical results (solid curve) and experimental data taken from Ref. [19] (circles).

The theoretical curve was found to coincide with the experimental results to an error of no greater than 2.7%.

Thus, one can note satisfactory agreement between theory and experiment with respect to the limiting behavior of the characteristics of convection for the lower part of a container filled with a fluid with internal heat sources.

5. Natural convection of heat-generating fluids in a quasi-two-dimensional geometry

In this section we discuss the characteristics of heat transfer from a heat-generating fluid confined to a model quasi-two-dimensional volume (Fig. 6). As in the case of the prototype volume, we denote the upper and lower boundaries of the quasi-two-dimensional volume by S_{up} and S_{dn}, respectively. The wide, plane vertical walls (whose size is of order $\sim R$) of the model volume are assumed to be thermally insulated. The thickness L of the quasi-two-dimensional container satisfies the inequality

$$L \ll R\,. \tag{5.1}$$

Strictly speaking, the heat-transfer distribution over the narrow section of the boundary of the quasi-two-dimensional volume differs from the corresponding distribution over the boundary of the original volume. Nevertheless, we can expect that, in certain conditions, these two distributions will be similar, at least qualitatively. In this section we will assess the maximum possible similarity in the heat-transfer distribution between the two types of volumes and establish the conditions in which such a similarity can be realized.

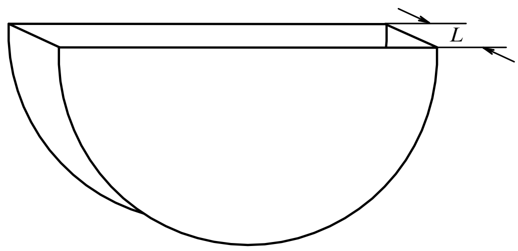

Figure 6. Model quasi-two-dimensional volume: L is the thickness of a vertical slice.

5.1 The best possible similarity in heat transfer between the quasi-two-dimensional model volume and the prototype volume

In view of inequality (5.1), the model slice volume is also close to a transverse slice of a long horizontal cylinder with the same cross-sectional area. We will widely use this fact in our further analysis, considering the long cylinder as an object intermediate between the original volume and its quasi-two-dimensional counterpart.

The thickness of the model volume is finite, thus limiting the convective motion of the fluid. This limitation is not important if the maximum thickness of the free-convection boundary layers that form in such a volume (at the wide vertical walls in particular) is small compared to the thickness of the cavity itself:

$$\delta_{\max} \ll L\,. \tag{5.2}$$

In the opposite limit, the constrained volume dramatically changes the structure of convective flow and, correspondingly, substantially modifies the characteristics of convective heat transfer in the quasi-two-dimensional volume compared to the cases of a long cylinder and, naturally, the prototype volume.

The general qualitative features of heat transfer inside a long horizontal cylinder are the same as for the prototype volume. For sufficiently large Rayleigh numbers, which correspond to well-developed convection, the temperature distribution over volume V_+ (see Fig. 1), bounded from below by the horizontal plane passing through the point of the maximum time-averaged temperature and from above by the plane section of the boundary, proves to be uniforms, due to turbulent mixing, irrespective of the shape of the volume. This implies that the character of the dependence of the Nusselt number for heat transfer through the upper boundary on the ordinary Rayleigh number is the same for the two geometries considered.

The situation is somewhat different for heat transfer through the lower boundary. Here the geometrical differences between the two types of volumes considered play an important role. Discrepancies are observed in the large-scale characteristics of the temperature and flow distributions within the boundary layer and the inner region V_-. Although these distributions are two-dimensional for both types of volumes, they are axisymmetric in the original volume and planar in the long horizontal cylinder. At the same time, these differences are quantitative rather than qualitative and may not affect the shapes of the dependences of the Nusselt number $\mathrm{Nu_{dn}}$ on the Rayleigh number and on the polar angle θ for $\theta \to 0$. In other words, the exponents in these dependences should be the same, although the numerical factors may differ. For the same reason, the critical Rayleigh numbers, which determine the transition from the laminar to the turbulent regime in the boundary layer (and, accordingly,, from one type of the dependence $\mathrm{Nu_{dn}}$ (Ra) to another) may also be different. The same refers to the characteristic values of the polar angle at which the limiting angular dependences established in Section 4 become valid. Finally, after we replace the ordinary Rayleigh number as the argument of the functional dependence of the Nusselt number by the modified Rayleigh number ($\mathrm{Ra} \to \mathrm{Ra_i}$), the difference between these two types of geometries also manifests itself in the numerical factors at the power laws for the heat transfer through the upper boundary.

Distinctive features of convection in the quasi-two-dimensional volume compared to the cases of the original volume and its cylindrical analog are, as noted above, the fact that the flow is restricted in the direction normal to the slice and the presence of viscous friction between the fluid and the vertical thermally insulated walls.

The adequacy of the heat-transfer model is conditioned by the distorting effects of these factors on the boundary-layer structure at the cooled sections of the boundary and on the heat- and mass-transfer patterns in the inner regions V_+ and V_-. These patterns, in turn, affect the characteristics of the boundary layers themselves.

If the effect of these two factors is insignificant (while condition (5.1) is satisfied), the heat-transfer characteristics in the two-dimensional geometry are close to those for the corresponding long cylinder, since the time-averaged convection is two-dimensional (planar) in both cases, whereas it is, as noted above, axisymmetric for the prototype volume.

This implies that the maximum possible similarity (in terms of heat transfer) between the model quasi-two-dimensional volume and the original volume reduces to the similarity between the long horizontal cylinder and the original volume. The necessary condition for such a similarity is given by inequality (5.2). Below we discuss this condition in greater detail.

5.2 Conditions for the best possible heat-transfer similarity between the model quasi-two-dimensional volume and the prototype volume

According to Section 4, the maximum thickness of the boundary layer at the cooled part of the boundary, $\delta_{\max}$, is attained at the pole. An estimate of this thickness, valid for $\mathrm{Ra_i} < 10^{17}$ and therefore important for the problem of nuclear-reactor safety, is given [according to equations (4.17) and (4.49)] by the expression

$$\frac{\delta_{\max}}{R} \propto \mathrm{Ra_i}^{-1/6} . \tag{5.3}$$

An estimate of the thickness of the shear boundary layer at the vertical thermally insulated walls in region V_+ follows from the general theory of shear boundary layers [7]:

$$\frac{\delta_+}{R} \propto \sqrt{\frac{\nu}{Ru_+}} . \tag{5.4}$$

Here, u_+ is the characteristic value of the large-scale pulsating flow velocity inside region V_+. This velocity is related to the characteristic amplitude of large-scale temperature pulsations in the same region via the estimate

$$u_+^2 \sim g\alpha\delta T_+ R , \tag{5.5}$$

which follows from the momentum balance condition.

One more relationship follows from the energy balance in the region V_+:

$$C\rho u_+ \delta T_+ \sim QR . \tag{5.6}$$

Combining (5.4) – (5.6), we arrive at an estimate for the thickness of the boundary layer at the thermally insulated walls in region V_+:

$$\frac{\delta_+}{R} \sim \mathrm{Ra_i}^{-1/6} . \tag{5.7}$$

The slowest flow in the entire volume is observed in the stable-stratification region V_-. Hence it would seem that the boundary layers that form at the thermally insulated walls should be the thickest ones and that such layers would lead to a strong distortion of the temperature distribution. However, the mechanism of formation of such boundary layers is quite different from the ordinary mechanism and therefore requires a special consideration. The point is that the internal sources additionally heat the fluid near the thermally insulated wall, where the viscous drag slows down the flow. The corresponding local rise in temperature leads, in turn, to an increase in the buoyancy force, which largely balances the viscous drag and acting as a feedback, limits the local rise in temperature. As a result, a peculiar temperature boundary layer is formed, which differs dramatically from the boundary layers considered above. Let us estimate the thickness of this layer, δ_-, and the temperature perturbation in it, δT_-.

If we allow for the balance between the viscous and buoyant forces, we get

$$\frac{\nu v_{\mathrm{v}}}{\delta^2} \sim g\alpha\delta T_- \,, \tag{5.8}$$

where v_{v} is the vertical component of the velocity outside the boundary layer in region V_-. Next, the requirement for energy balance in the boundary layer yields the estimate

$$\frac{\lambda\delta T_-}{\delta_-^2} \sim Q \,. \tag{5.9}$$

Eliminating δT_- from (5.8) and (5.9) yields

$$\delta_- \sim \left(\frac{\lambda\nu v_{\mathrm{v}}}{g\alpha Q}\right)^{1/4} . \tag{5.10}$$

We substitute the estimate that follows from equation (4.36),

$$\rho C v_{\mathrm{v}} \frac{T}{z} \sim Q \,, \tag{5.11}$$

into (5.10) to obtain

$$\delta_- \sim \left(\frac{\nu\chi z}{g\alpha T}\right)^{1/4} . \tag{5.12}$$

Finally, using the estimate

$$T \sim T_{\max}\left(\frac{z}{H}\right)^{4/5} \tag{5.13}$$

that can be obtained from (4.44) and expressing $T_{\max}$ in terms of the thickness δ of the boundary layer at the cooled wall for vertical coordinates $z \sim H$, we arrive at an estimate for the thickness of the temperature boundary layer at the vertical thermally insulated walls in the region V_- of the quasi-two-dimensional volume:

$$\delta_- \sim \delta\left(\frac{z}{H}\right)^{1/20} < \delta_{\max} \,. \tag{5.14}$$

From (5.9) and (5.10), in the same manner as in deriving (5.14), we obtain an estimate for the temperature perturbation in the boundary layers at the vertical thermally insulated walls in the region V_- of the quasi-two-dimensional volume:

$$\delta T_- \sim T\frac{\delta}{H}\left(\frac{H}{z}\right)^{7/10} . \tag{5.15}$$

This estimate suggests that temperature perturbations are small at $z > \delta$.

From a comparison of the estimates (5.3), (5.7), and (5.14), we see that the maximum thickness of the boundary layer in the quasi-two-dimensional volume is attained in the cooled part of the boundary at the pole. Hence, in accordance with the requirement (5.2) and the estimate (5.3), we finally arrive at the condition for the maximum similarity in heat transfer between the quasi-two-dimensional volume and the prototype volume:

$$\frac{L}{R} \gg \mathrm{Ra}_{\mathrm{i}}^{-1/6} . \tag{5.16}$$

This inequality should be considered a criterion for the maximum possible similarity between the model quasi-two-dimensional volume and the prototype volume.

In the range of modified Rayleigh numbers most important for the problem of safety of nuclear reactors, $\mathrm{Ra}_{\mathrm{i}} \sim 10^{12} - 10^{17}$, condition (5.16) corresponds to the requirement $L/R \gg 10^{-2}$, which, as a rule, can be satisfied in practice without difficulties.

Table 3 lists the minimum values of the L/R ratio, the ranges of variation of the number Ra_{i}, and the maximum value of $\mathrm{Ra}_{\mathrm{i}}^{-1/6}$ realized in the four known quasi-two-dimensional experiments. Clearly, the most favorable parameter ratio [in terms of the satisfaction of criterion (5.16)] was achieved in the BALI experiments and the least favorable in Stainbrenner and Reineke's experiment.

Table 3. Parameters of experiments carried out in a quasi-two-dimensional geometry.

	$(L/R)_{\min}$	Ra_{i}	$(\mathrm{Ra}_{\mathrm{i}}^{-1/6})_{\max}$
Mayinger et al. [16, 19, 20]	0.13	$10^7 - 5\times10^{10}$	5×10^{-2}
Stainbrenner and Reineke [21]	0.044	$5\times10^{12} - 1.0\times10^{14}$	0.8×10^{-2}
COPO [25, 26]	0.125	$3\times10^{14} - 2\times10^{15}$	3.8×10^{-3}
BALI [28]	0.1	$10^{15} - 10^{17}$	0.32×10^{-2}

6. Particularities of convection in a cooling-down fluid without internal heat sources

6.1 Preliminary analysis

Since the thickness of the boundary layer at large Rayleigh numbers is much smaller than the characteristic size of the volume occupied by the fluid, the flow velocities in the boundary layer are, as follows from the mass-balance condition, much higher than the velocities in the bulk of the volume. However, it is the latter that determine the characteristic cooling time. Hence the rate of the convective processes in the boundary layer (which determine the heat resistance to the heat flux at the boundary) is much higher than the cooling rate; therefore, the process can be assumed to be quasi-steady-state. Thus, Theofanous and Liu [29] suggested that the heat removal from a cooling-down fluid without internal heat sources is equivalent to the heat removal from a fluid with uniformly distributed heat sources (in a steady-state regime). In this section, we analyze this suggestion more thoroughly.

We retain all assumptions on the shape of the fluid volume adopted in Sections 3 and 4 (and also in Figs 1 and 2). We also use the previously introduced notation.

The changes in the thermal energy of a cooling-down fluid are largely similar to the effects of internal heat sources. Formally this is reflected by the fact that, for quasi-steady-state processes, the term with the time derivative in the energy-balance equation, when taken with the opposite sign, can be regarded as the effective power density of heat release:

$$\widetilde{Q} \equiv -C\rho\,\frac{\partial T}{\partial t} \,. \tag{6.1}$$

This is sufficient to conclude that the effective power density is distributed uniformly only in that part of the volume where the time average of the fluid temperature is also uniform. This part is region V_+ (see Fig. 1) situated above the maximum of the time-averaged temperature in the fluid volume. On the other hand, in region V_- (below the maximum of the time-averaged temperature), the thermal stratification is stable, and there the effective source-power density $\widetilde{Q}$ is definitely nonuniform, in accordance with (6.1). This, in turn, means that the temperature distribution in V_- should be different for fluids of the two types. Alternatively, this can be ascertained by means of qualitatively considering the mechanisms of the formation of the temperature distribution in the region at hand.

In a heat-generating fluid, the heating-up of particles traveling between two points situated at different heights in V_- is proportional to the traveling time. In contrast, in a cooling-down fluid without internal heat sources, where heat and mass transfer is time-dependent, the temperatures at two analogous points coincide provided they refer to different moments separated by the time interval taken by these particles to travel between the points. Naturally, differences in the temperature distributions in the bulk of volume V_- for fluids of the two types leads to differences in the heat-flux distribution over the lower boundary (see Fig. 1). Below we concentrate on the special features of the distribution of the heat transfer from a cooling-down fluid without internal heat sources over the lower boundary at polar angles $\theta \ll 1$ (see Fig. 2), where the difference between the two types of fluids is especially significant. As in the case of a heat-generating fluid, this distribution is a solution to the combined problem on convection in the boundary layer and in the adjacent region of the bulk volume.

The main qualitative features of the boundary layer for a cooling-down fluid without internal heat sources at the lower section of the boundary at $\theta \ll 1$ coincide with those for a heat-generating fluid examined in the preceding section. The boundary layer is convergent, it slows down and satisfies the same boundary condition (4.1) and the conditions of matching to the characteristics of the bulk volume, (4.2) and (4.3). In view of the quasi-steady-state nature of the boundary-layer processes in a cooling-down fluid, the relevant equations of motion coincide with those for the boundary layer in a heat-generating fluid. Hence most relations obtained from the analysis of the boundary layer in the preceding section remain valid for a cooling-down fluid, including (4.13), (4.14), (4.27), and (4.28), which we will use in our further analysis.

6.2 Convection in the bulk volume and the heat flux distribution over the boundary

In the bulk volume, where viscosity and heat conduction are insignificant, the momentum and energy balance conditions for a cooling-down fluid without internal heat sources assume the form

$$\frac{\partial \mathbf{v}_{\mathrm{b}}}{\partial t} + (\mathbf{v}_{\mathrm{b}}\,\mathrm{grad})\mathbf{v}_{\mathrm{b}} = -\frac{\mathrm{grad}\,p}{\rho} + g\alpha T_{\mathrm{b}}\mathbf{n}\,, \tag{6.2}$$

$$\frac{\partial T_{\mathrm{b}}}{\partial t} + (\mathbf{v}_{\mathrm{b}}\,\mathrm{grad})T_{\mathrm{b}} = 0\,. \tag{6.3}$$

Specific features of these equations are the absence of terms representing heat sources in equation (6.3) and the presence of time derivatives in both equations.

The analysis of the system (6.2), (6.3) that completely reproduces the analysis given in Section 4 for the system (4.29), (4.30) suggests that, at $z \gg \delta$, the temperature and the vertical component of velocity in the bulk volume are virtually independent of the horizontal coordinates. As a result, equation (6.3) becomes

$$\frac{\partial T_{\mathrm{b}}}{\partial t} + v_{\mathrm{v}}\,\frac{\partial T_{\mathrm{b}}}{\partial z} = 0\,. \tag{6.4}$$

It follows from (4.13) and (4.27) that the dependence ofv_{b} on the z coordinate is much weaker than the dependence of the function $T_{\mathrm{b}}(z,t)$, and can be neglected. Then the solution of equation (6.4) obtained by the method of characteristics can be written as

$$T_{\mathrm{b}}(z,t) = T_0\left(t - \frac{z}{v_0(t)}\right), \tag{6.5}$$

where $T_0(t)$ and $v_0(t)$ are, respectively, the temperature (measured from the temperature at the boundary) and the vertical component of velocity in the bbulk volume at the vertical coordinate $z \approx \delta$.

The time dependence of $T_0(t)$ can be described by the equation

$$\frac{\partial T_0}{\partial t} = -\frac{T_0}{\tau(t)}\,, \tag{6.6}$$

which follows from the energy balance condition for the entire fluid volume. The reciprocal of the cooling time, $\tau^{-1}(t)$, is proportional to the Nusselt number averages over the boundary in a way, $\mathrm{Nu} \sim \mathrm{Ra}^s$, where the exponent s is much smaller than unity $(1/4 < s < 1/3)$. Since $\mathrm{Ra} \sim \Delta T$, the function $\tau(t)$ in (6.6) satisfies the inequality

$$\frac{\mathrm{d}\tau}{\mathrm{d}t} \ll 1\,. \tag{6.7}$$

In view of (6.7), equations (6.5) and (6.6) imply that the temperature distribution in the bulk volume can be written as

$$T_{\mathrm{b}}(z,t) = T_0(t)\exp\left(\frac{z}{v_0(t)\tau(t)}\right). \tag{6.8}$$

It follows from (4.13), (4.27), and (6.8) that

$$\frac{v_{\mathrm{b}}(z,t)}{v_0(t)} \sim \exp\left(\frac{z}{m v_0(t)\tau(t)}\right), \tag{6.9}$$

where $m = 4$ for the laminar boundary-layer regime, and $m = 9/4$ for the turbulent regime.

Expressions (6.8) with (4.14) and (4.28) taken into account allow us to represent the distributions of temperature in the bulk volume and of the heat-flux density at the boundary in the form

$$T_{\mathrm{b}}(z,t) = T_0(t)\exp\left(k\,\frac{z}{R}\right), \tag{6.10}$$

$$q(\theta,t) = q_{\min}(t)\exp\left(p\theta^2\right), \tag{6.11}$$

where k and p are dimensionless quantities and $q_{\min}$ is the minimum heat flux density at the boundary (realized at $\theta = 0$). Since

$$\frac{v_{\mathrm{b}}(R,t) - v_0(t)}{v_0(t)} \sim 1$$

we conclude from (6.9) that the product $v_0(t)\tau(t)$ is much smaller than R; therefore, k and p in (6.10) and (6.11) should be much larger than unity. Moreover, these quantities for the turbulent regime in the boundary layer should be smaller than for the laminar regime.

6.3 Discussion and comparison with experiment

According to equations (6.10) and (6.11), for moderate values of the arguments, the temperature in the stable-stratification region as a function of height and the heat-flux density as a function of the square of the polar angle are of exponential form. The scale of the height dependence of temperature is much smaller than the curvature radius of the boundary near the pole, and the scale of the polar-angle dependence of the heat flux density is much smaller than unity. Hence, even at $\theta \ll 1$ and $z \ll H$ ($H \sim R$ is the height of the fluid volume), the exponential nature of the dependences is quite pronounced. The rate of the exponential growth depends on the flow regime in the boundary layer: it is higher for the laminar regime. Since at small values of the polar angle the boundary-layer flow slows down, the flow regime finally becomes laminar there, and the exponential dependence becomes steeper. Let us now compare the theoretical result obtained here for the heat-flux distribution $q(\theta)$ with experiment.

In their experiments with the ACOPO facility, Theofanous and Liu [29] measured the heat-flux-density distribution over the boundary. The experimental data were represented in the form of a dependence of the reduced heat-flux density

$$Y = \frac{q(\theta)}{q_{\mathrm{dn}}} \tag{6.12}$$

on the reduced angle

$$X = \frac{\theta}{\theta_0}\,, \tag{6.13}$$

where q_{dn} is the heat-flux density averaged over the lower boundary and θ_0 is the angular position of the upper boundary to which the fluid fills the model container. The experimental dependence $Y = Y(X)$ in Ref. [29] was interpolated by polynomials separately in two regions: by a third-power polynomial for $0.1 < X < 0.6$ and by a second-power polynomial for $0.6 < X < 1$. Let us compare theoretical and experimental results.

If we assume that equation (6.11) is valid for $X < 0.6$, the theoretical relationship between the reduced heat flux density and reduced polar angle can be written as

$$Y = a \exp(bX^2)\,, \tag{6.14}$$

where a and b are constants (adjustable parameters). The choice

$$a = 0.1658\,, \quad b = 4.987 \tag{6.15}$$

led to agreement between the theoretical dependence and experimental data with a discrepancy of about 3.4%. Note that b in (6.15) obtained by comparison with experiment proved to agree with the above-presented theory, according to which the parameter p in equation (6.11) should be much larger than unity. The results of the comparison are depicted in Fig. 7.

Note that, in contrast to the exponential dependence (6.14) theoretically obtained here, the polynomial interpolation used by Theofanous and Liu [29] does not seem to be natural, since the numerical factors in the polynomials alternate in sign and are large in absolute value [see formulas (2.11)].

In conclusion, we note that, irrespective of similarities between convection in a cooling-down fluid without internal heat sources and convection in a heat-generating fluid, there is a substantial difference between these two cases in what concerns the heat-flux distribution at the boundary and the temperature distribution in the bulk volume. As we have seen, for a cooling-down fluid these distributions are exponential, while for a heat-generating fluid they are power functions, in accordance with the theoretical and experimental results (see Section 4).

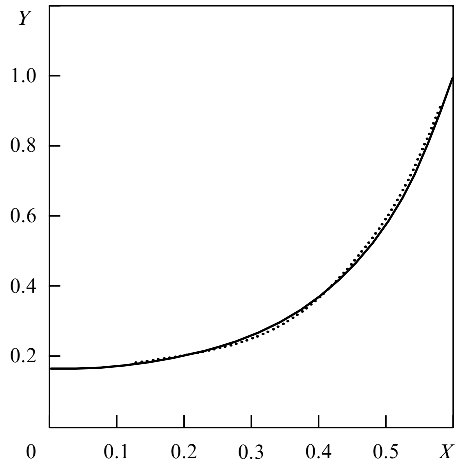

Figure 7. Polar-angle dependence of heat flux: comparison of theory (solid curve) and experiment (dotted curve).

7. Conclusion

The ideas formed on the basis of theoretical and experimental studies of the structure of natural convection in a one-component fluid with internal heat sources confined to a closed volume are as follows.

There are four basic and one asymptotic heat-transfer regime. They differ in the type of convection in the upper part of the volume and in the boundary layer at the lower section of the boundary. Each regime corresponds to a certain combination of exponents in the power dependences of the Nusselt numbers for heat transfer through the upper and lower boundaries on the dimensionless strength of heat generation — the modified Rayleigh number.

In the range of strengths ($\mathrm{Ra_i} = 10^4 - 10^{17}$) in which experiments were conducted, convection regimes of hard turbulence are realized in the upper part of the volume. In the range of moderate strengths of heat generation ($\mathrm{Ra_i} = 10^4 - 10^{12}$), a laminar regime sets in in the boundary layer at the lower boundary. In this case, the fraction of heat transfer through the upper boundary increases slowly with the power of heat generation ($\gamma_{\mathrm{up}} > \gamma_{\mathrm{dn}}$). At very high powers, the type of convection changes in the lower boundary layer from laminar to turbulent. As a result, as the power increases at $\mathrm{Ra_i} > 10^{13} - 10^{14}$, a tendency for an increase in the lower-boundary fraction of heat transfer appears if $\gamma_{\mathrm{dn}} > \gamma_{\mathrm{up}}$.

For $\mathrm{Ra_i} \gg 1$, the power of heat release within the boundary layer as a whole is much smaller than the heat fluxes passing through the layer. Hence, if we restrict ourselves to the heat-transfer distribution between the upper and lower boundary, we find that in both fragments of the volume of the heat-generating fluid — the upper part of the volume and the lower boundary layer — convection is similar to that in a fluid without internal heat sources. This fact and the use of the energy balance condition made it possible to determine the numerical values of the exponents γ_{up} and γ_{dn} for all heat-transfer regimes, which proved to be close to the experimental results.

The situation changes dramatically if we examine the detailed characteristics of the heat-transfer distribution over the lower part of the boundary. Here, as the lowest point of the boundary (the pole) is approached, the boundary layer acquires properties that have no simple analogs in the convection of a fluid without internal heat sources. The boundary layer becomes convergent, it slows down, and returns the fluid to the bulk of the volume. The temperature distribution in the bulk, outside the boundary layer, proves to be stably stratified. The characteristics of convection in the convergent boundary layer and in the adjacent bulk are interrelated. Solutions to the corresponding self-consistent problem led to the experimentally corroborated conclusion that the height dependence of the heat-flux density at the boundary on the polar angle measured from the pole and the height dependence of the bulk temperature bulk are power functions, generally, with fractional exponents.

The characteristics of heat transfer in a vertically oriented axisymmetric volume and in a thin central vertical slice of such a volume may closely correspond to each other for a certain limitation from below on the thickness of the slice; this restriction weakens as the power of heat generation increases.

In many respects, the characteristics of heat transfer in a cooling-down fluid without internal heat sources are similar to those for a heat-generating fluid. However, there is a fundamental difference in the distribution of heat transfer through the lower boundary between the two types of fluids: the polar-angle dependence of the heat-flux density for the cooling-down fluid is an exponential rather than a power function typical of a heat-generating fluid. This difference imposes certain limitations on the use of experiments with a cooling-down fluid without internal heat sources for simulating heat transfer in a heat-generating fluid.

The authors express their gratitude to A M Dykhne and A I Leont'ev for interesting discussions of the material of the present review.

References

1. Bénard H *Revue Gen. Sci. Pures Appl.* **11** 1261, 1309 (1900)
2. Rayleigh J W *S Philos. Mag.* **32** 529 (1916)
3. Prandtl L Z *Angew. Math. Mech.* **5** 136 (1925)
4. Prandtl L Z *Ver Deut. Ing.* **77** 105 (1933)
5. Von Kármán T *Trans. ASME* **61** 705 (1939)
6. Kolmogorov A N *Dokl. Akad. Nauk SSSR* **30** 299 (1941)
7. Landau L D, Lifshitz E M *Mekhanika Sploshnykh Sred* (Fluid Mechanics) (Moscow: Nauka, 1986) [Translated into English (Oxford: Pergamon Press, 1987)]
8. Zel'dovich Ya B *Zh. Eksp. Teor. Fiz.* **12** 1463 (1937)
9. Kutateladze S S *Osnovy Teorii Teploobmena* (Fundamentals of Heat Transfer Theory) (Moscow: Nauka, 1979)
10. Spalding D B, Afgan N (Eds) *Heat Transfer and Turbulent Buoyant Convection* Vol. 1, 2 (Washington: Hemisphere Publ. Corp., 1977)
11. Kakač S, Aung W, Viskanta R (Eds) *Natural Convection: Fundamentals and Applications* (Washington: Hemisphere Publ. Corp., 1985)
12. Cebeci T, Bradshaw P *Physical and Computational Aspects of Convective Heat Transfer* (New York: Springer, 1984) [Translated into Russian (Moscow: Mir, 1987)]
13. Gebhart B et al. *Buoyancy-Induced Flows and Transport* (Washington, D.C.: Hemisphere Publ. Corp., 1988) [Translated into Russian (Moscow: Mir, 1991)]
14. Theofanous T G, in *Multiphase Flow 1995. Proc. of the Second Intern. Conf.* (Eds A Serizawa, T Fukano, J Bataille) (Amsterdam: Elsevier, 1995) p. 573
15. Kulacki F A, Goldstein R J *J. Fluid Mech.* **55** (Pt. 2) 271 (1972)
16. Mayinger F X, Jahn M, Reineke H H, Stainbrenner U, BMFT, RS 48/1 (Hannover, FRG: Institute für Verfahrenstechnik der T.U., 1976)
17. Kulacki F A, Emara A A *J. Fluid Mech.* **83** (Pt. 2) 275 (1977)
18. Kulacki F A, Nagle M E *J. Heat Transfer* **91** 204 (1975)
19. Jahn M "Holografische Untersuchung der freien Konvektion in volumetrisch beheiten Fluiden", Doktor-Ingenieur Dissertation (Hannover, 1975)
20. Mayinger F X, Fritz P, Reineke H H et al., Technical Report FT-FB RS 166-79-05 (Bonn: Bundesministerium für Forschung und Technologie, 1980)
21. Stainbrenner U, Reineke H H, in *Proc 6-th Int. Heat Transfer Conf.* Vol. 2 (Toronto, 1978) p. 305
22. Alvarez D, Malterre P, Seiler J *BNFS* (London, 1986) p. 331
23. Asfia F J, Dhir V K, in *Proc. of the Workshop on Large Molten Pool Heat Transfer* (Grenoble, NEA/CSNI/R(94) 11) (Paris: OECD Nucl. Energy Agency, 1994) p. 229
24. Frantz B, Dhir V K *ASME* **192** 69 (1992)
25. Kymäläinen O, Hongisto O, Tuomisto H, Theofanous T G, in *Proc. of the Workshop on Large Molten Pool Heat Transfer* (Grenoble, NEA/CSNI/R(94)11) (Paris: OECD Nucl. Energy Agency, 1994) p. 199
26. Kymäläinen O et al. *Nucl. Eng. Des.* **149** 401 (1994)
27. Helle M, Kymäläinen O, Tuomisto H, in *OECD/CSNI Workshop on In-Vessel Core Debris Retention and Coolability* (Garching, NEA/CSNI/R(98)18) (Paris: OECD Nucl. Energy Agency, 1999) p. 173
28. Bonnet J-M, Seiler J-M, in *7-th Int. Conf. on Nucl. Engineering ICONE-7057* (Tokyo, 1999)
29. Theofanous T G, Liu C, in *Proc. American Nucl. Soc. National Heat Transfer Conf.* (Portland, Oregon, 1995) p. 349
30. Theofanous T G et al., in *Proc. PSA '96-Int. Topical Meeting on Probabilistic Safety Assessment* (Park City, Utah, 1996) p. 1343
31. Theofanous T G, Angelini S, in *Proc. Eighth Intern. Topical Meeting on Nuclear Reactor Thermal-Hydraulics: NURETH-8* (*Kyoto, Japan, 1997*) (Tokyo: Atomic Energy Soc. Japan, 1997) p. 165
32. Kelkar K M, Schmidt R C, Patankar S V, in *Proc. Int. Heat Transfer Conf.* (San Diego, USA, 1991) p. 355
33. Churbanov A G et al. *Int. J. Heat Mass Transfer* **37** 2969 (1994)
34. Bolshov L A et al. *Nucl. Sci. J.* **32** 134 (1995)
35. Dinh T N, Nourgaliev R R *Nucl. Eng. Design* **169** 131 (1997)
36. Nourgaliev R R et al., in *OECD/CSNI Workshop on In-Vessel Core Debris Retention and Coolability* (Garching, NEA/CSNI/R(98)18) (Paris: OECD Nucl. Energy Agency, 1999) p. 215
37. Chudanov V V et al., in *OECD/CSNI Workshop on In-Vessel Core Debris Retention and Coolability* (Garching, NEA/CSNI/R(98)18) (Paris: OECD Nucl. Energy Agency, 1999) p. 223
38. Bolshov L A, Kondratenko P S, Strizhov V F, in *Proc. of the Intern. Symp. on Transient Convective Heat Transfer* (Cesme, Turkey, August 19–23, 1996) (New York, Vallingford (UK), 1997) p. 103
39. Bolshov L A, Kondratenko P S, Strizhov V F *Int. J. Heat Mass Transfer* **41** 1223 (1998)
40. Bol'shov L A, Kondratenko P, in *Trudy Vtoroĭ Rossiĭskoĭ Natsional'noĭ Konferentsii po Teploobmenu* (Proc. 2nd Russian National Conference on Heat Transfer) Vol. 3 (October 26–30, 1998) (Moscow, 1998) p. 50
41. Bolshov L A, Kondratenko P S, Strizhov V F, in *OECD/CSNI Workshop on In-Vessel Core Debris Retention and Coolability* (Garching, NEA/CSNI/R(98)18) (Paris: OECD Nucl. Energy Agency, 1999) p. 235
42. Bolshov L A, Kondratenko P S, in *Proc. of the 1999 NURETH-9 Conf.* (San Francisco, California, 1999) Log 304
43. Bolshov L A, Kondratenko P S, Strizhov V F, in *Proc. of the 1999 NURETH-9 Conf.* (San Francisco, California, 1999) Log 305
44. Bolshov L A, Kondratenko P S *Int. J. Heat Mass Transfer* **43** 3897 (2000)
45. Chawla T C, Chan S H *J. Heat Transfer* **104** 465 (1982)
46. Catton I, Edwards D K *J. Heat Transfer* **89** 295 (1967)
47. Castaing B et al. *J. Fluid Mech.* **204** 1 (1989)
48. Wu X-Z, Libchaber A *Phys. Rev. A* **45** 842 (1992)
49. Kutateladze S S, Berdnikov V S *Int. J. Heat Mass Transfer* **27** 1595 (1984)
50. Bejan A, Gunnington G R *Int. J. Heat Mass Transfer* **24** 131 (1983)
51. Mahajan R L, Gebhart B *J. Fluid Mech.* **91** 131 (1979)
52. Bejan A, in *Natural Convection: Fundamentals and Applications* (Eds S Kakač, W Aung, R Viskanta) (Washington: Hemisphere Publ. Corp., 1985) p. 75
53. Vliet G C, Liu C K *J. Heat Transfer* **91** 517 (1969)
54. Cheung F B *J. Fluid Mech.* **97** 743 (1980)
55. Chu T Y, Bentz J H, Simpson R B *AIChE Symp. Ser.* **91** 154 (1995)
56. Himasekhar K "An Analytical and Experimental Study of Laminal Free Boundary Layer Flows in a Stratified Medium", Thesis (India: I.I.T. Kanpur, 1980)